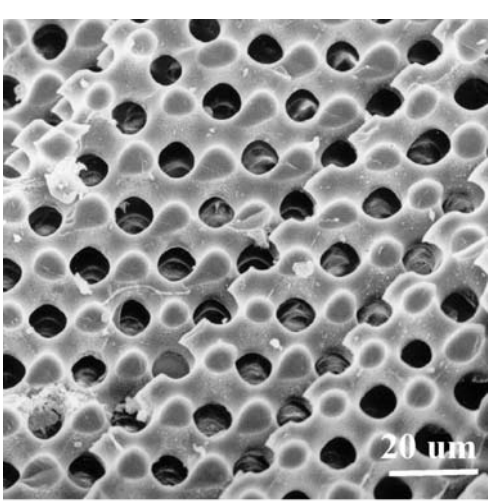
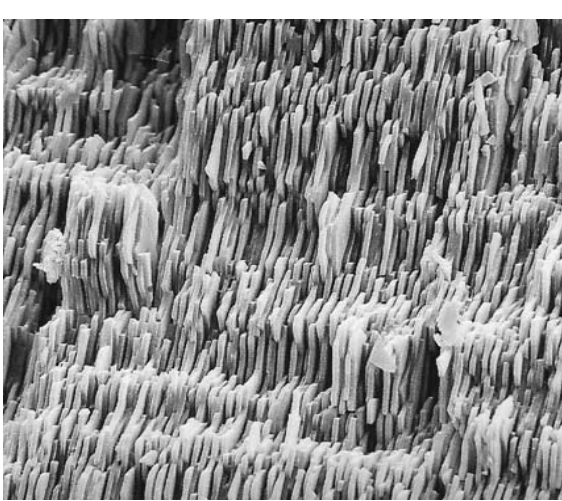
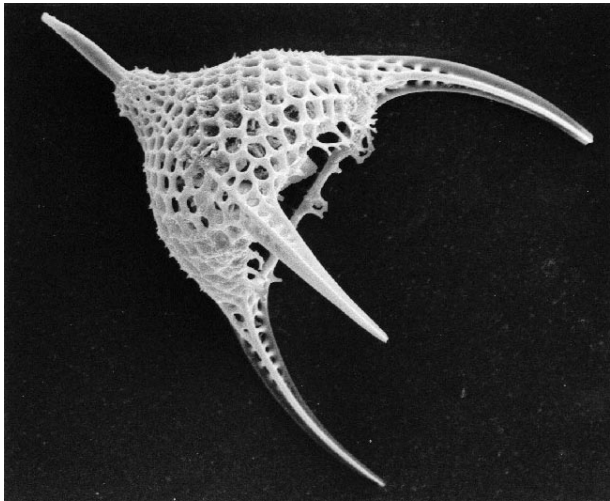
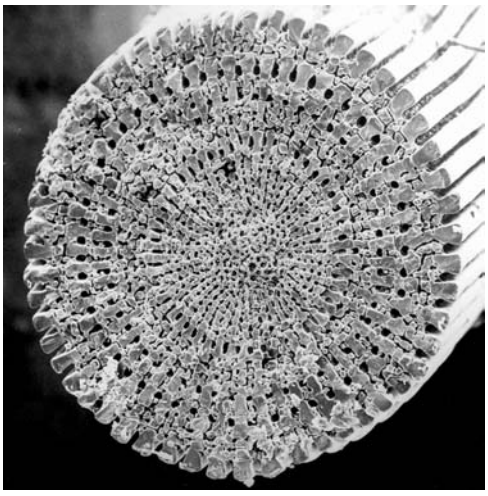
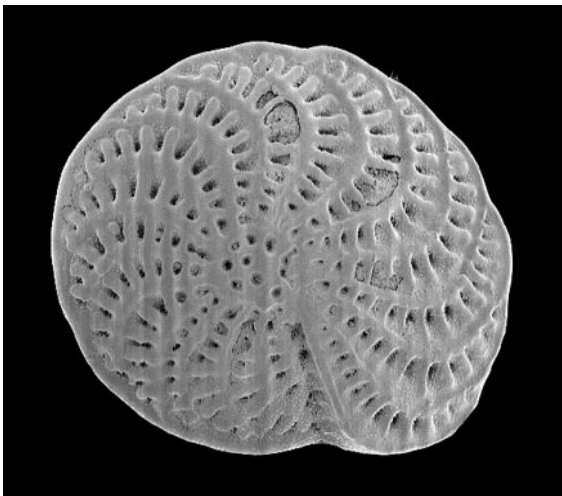
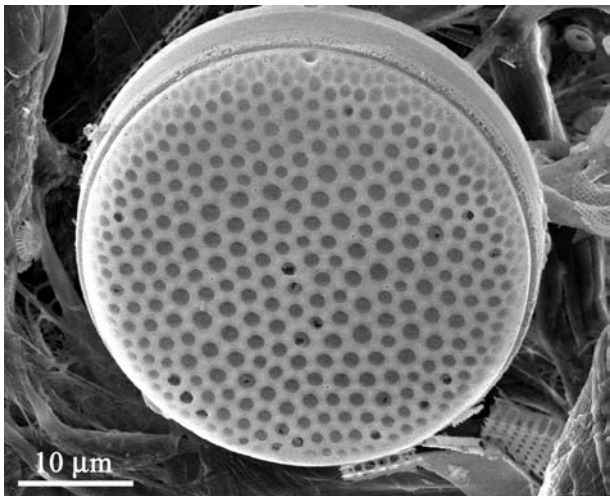


Mineral Morphologies

Fiona Meldrum

School of Chemistry,
University of Bristol, UK

Biomineralisation



AMORPHOUS

POLYCRYSTALLINE

SINGLE CRYSTAL

Introduction

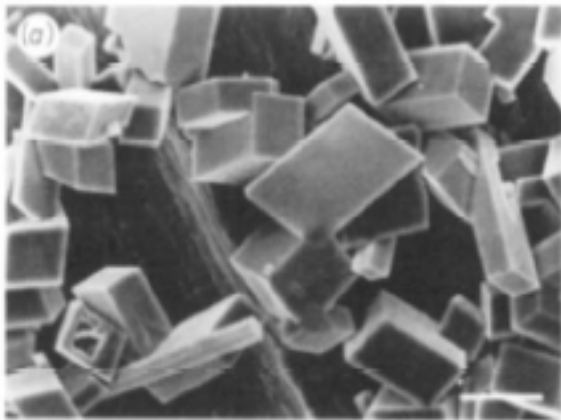
Routes to Controlling Crystal Morphologies:

- Additives to control single crystal morphologies
- Additives to produce polycrystalline structures
 - ⇒ Oriented and non-oriented
- Templating to control production :
 - ⇒ Nanoparticles
 - ⇒ Polycrystalline structures with complex morphologies
 - ⇒ Single crystals with complex morphologies

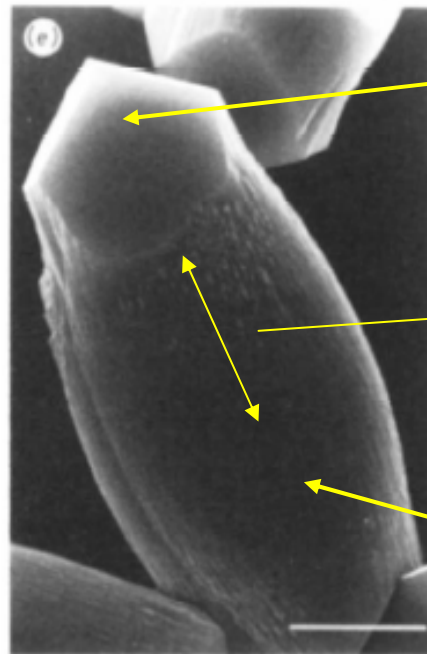
Additives to Control Single Crystal Morphologies

Calcite Precipitation in the Presence of α,ω -Dicarboxylates

- Influence of subtle changes in additive structure studied
- Malonic acid ($n = 1$) was the most effective \Rightarrow effect reduced with increasing chain length



Control



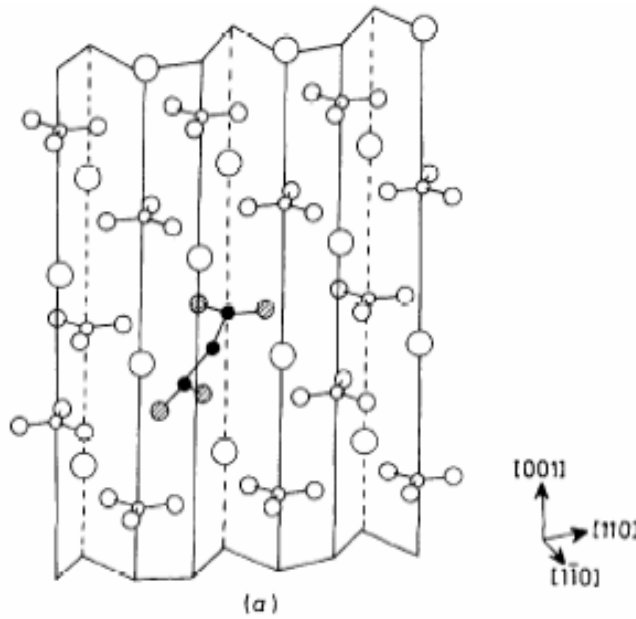
Ca/malonate 1:3

capped with
rhombohedral {104}
end faces

elongated parallel
to the c -axis

curved {1-10}
faces

- Morphological changes were considered in terms of molecular recognition between the crystal face and additive
- Calcite crystal faces parallel to the c -axis have carbonate groups oriented perpendicular to the face
- These faces may be stabilised via stereoselective adsorption of the acids via bidentate binding of the carboxylate groups



(1-10) face of calcite showing possible malonate binding site

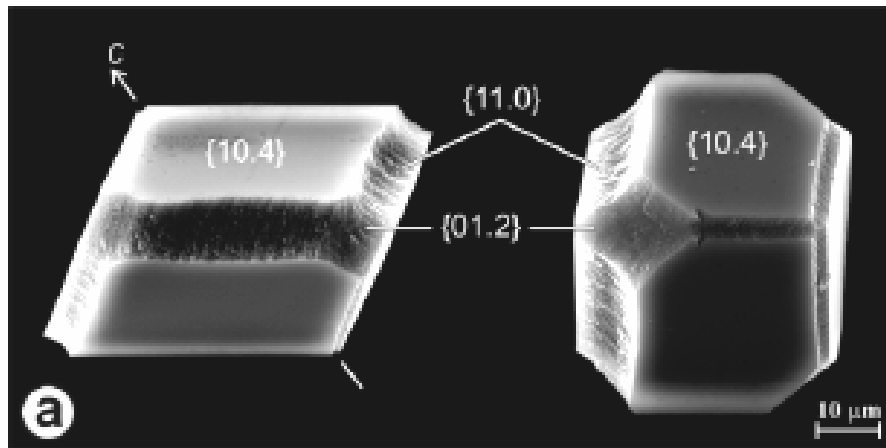
Cooperative binding of the carboxylate groups may occur in the case of the short-chain additives

The carboxylate groups in the longer-chain additives behave independently

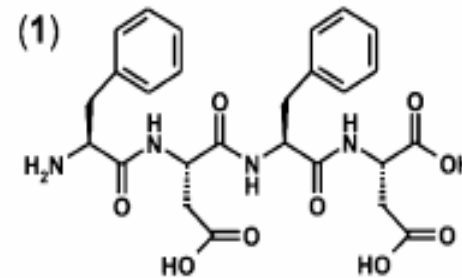
Acidic Peptides as Growth Modifiers

Acidic proteins extracted from biogenic CaCO_3 often comprise alternating Asp or Glu residues and more hydrophobic residues.

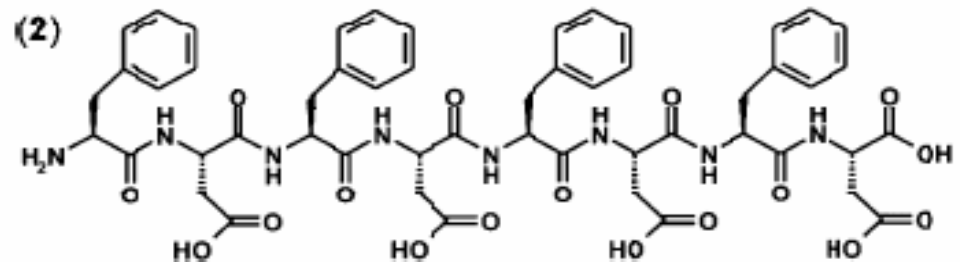
⇒ Mimic this structure / use as calcite growth modifier



H-(Phe-Asp)₂-OH



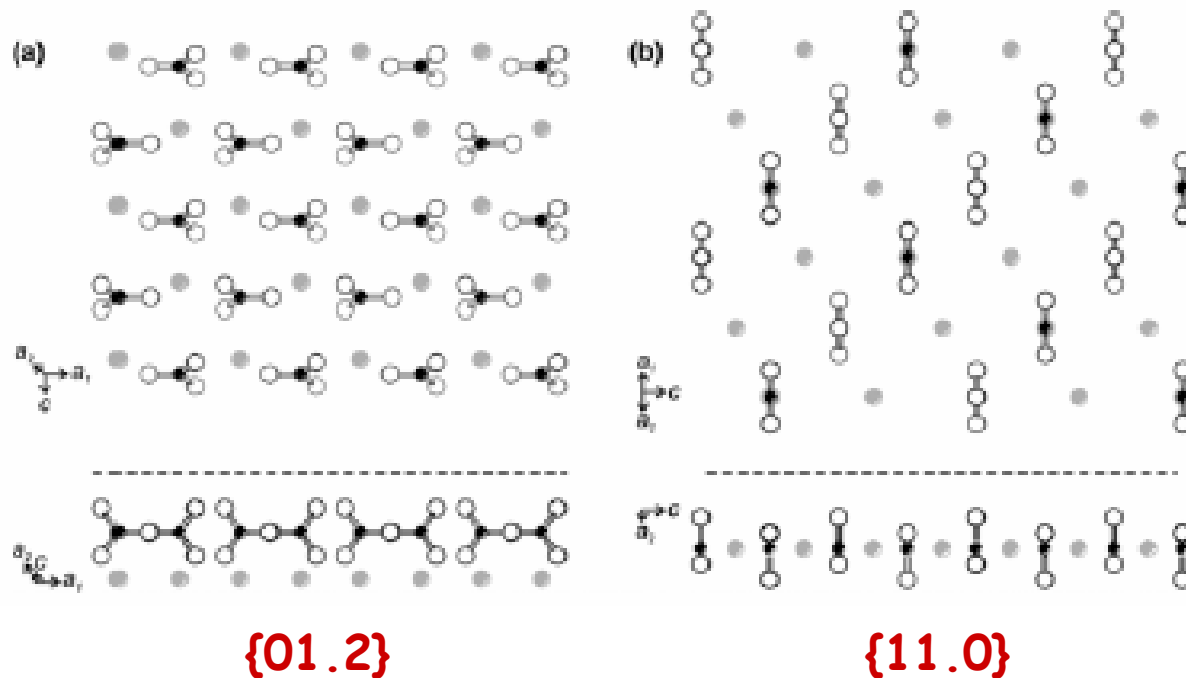
H-(Phe-Asp)₄-OH



Observe NEW {01.2}
and {11.0} faces

$\{01.2\}$ and $\{11.0\}$ faces have few common features in terms of symmetry or electrostatics

Also, polymer additives **very flexible**



\Rightarrow Seems unlikely these faces are selected on the basis of stereochemical or geometrical recognition

Additives to Control Polycrystalline Particle Morphologies

Higher concentration of additives

- ⇒ Observe transition from single crystal to polycrystalline structure
- ⇒ Can obtain unusual morphologies

Polycrystalline particles frequently form by aggregation

- ⇒ Can be disordered or oriented
- ⇒ Aggregation can be mediated by additives

Aggregation-Based Crystal Growth

In natural systems (biology, geology), crystal growth traditionally considered to occur by:

- 1 Atom-by-atom addition
- 2 Dissolution of unstable phases and reprecipitation as more stable phases

However...

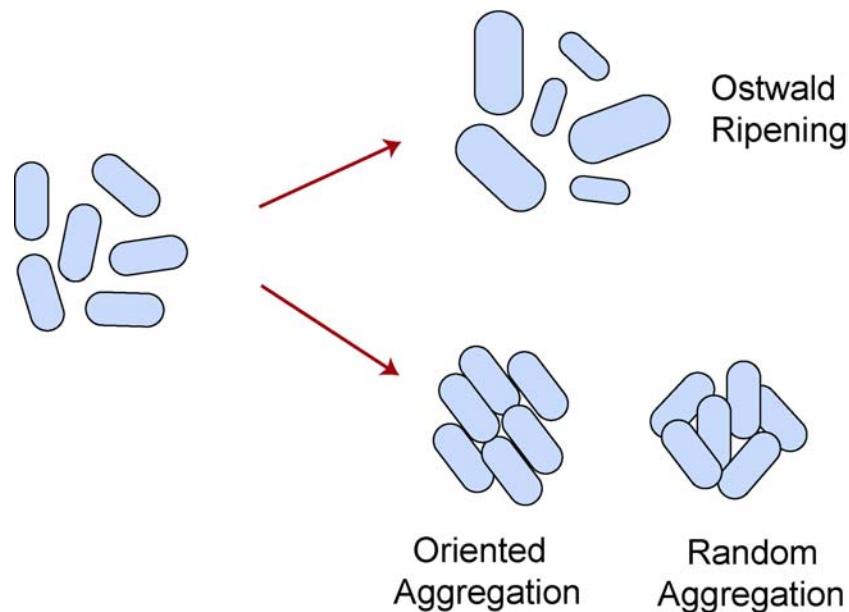
There is growing evidence that **self-assembly based mechanisms** may also be very widespread

Nanosized particles can also provide the building blocks for the growth of ordered solids

Growth by Aggregation

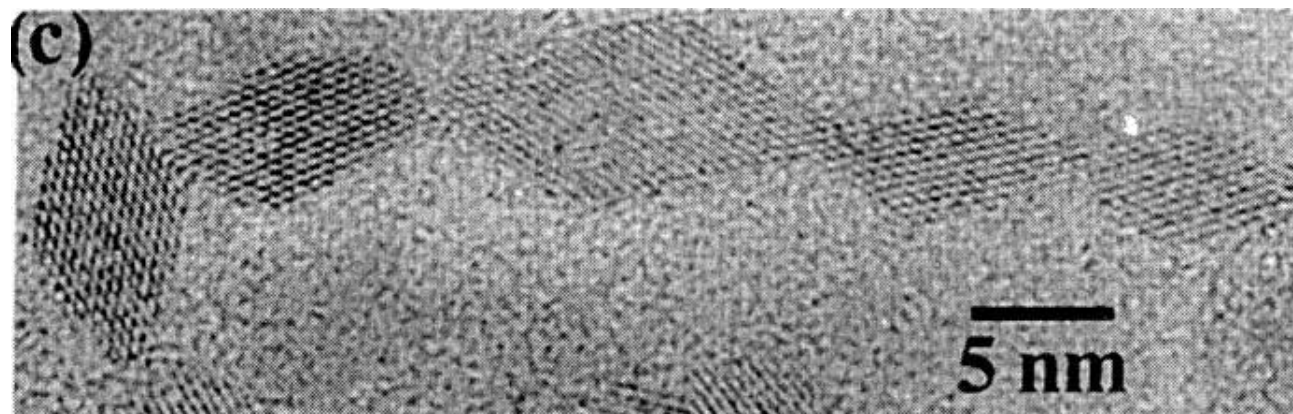
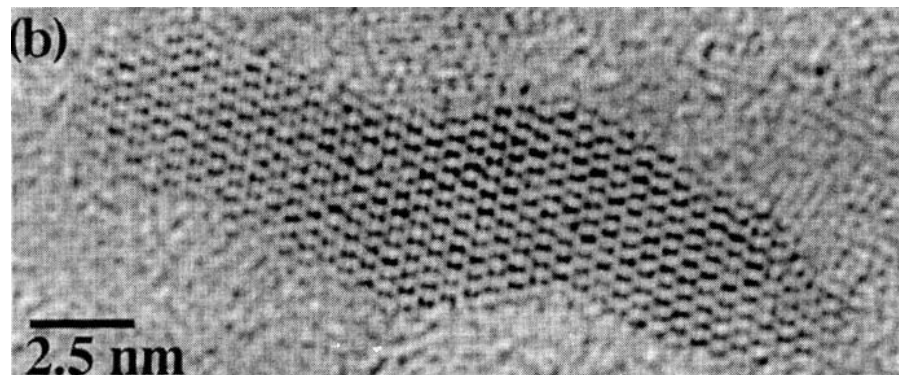
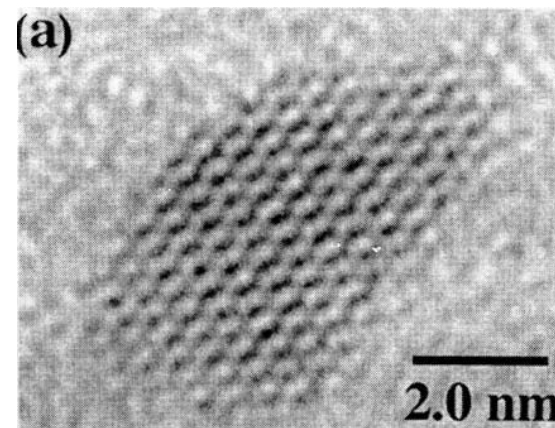
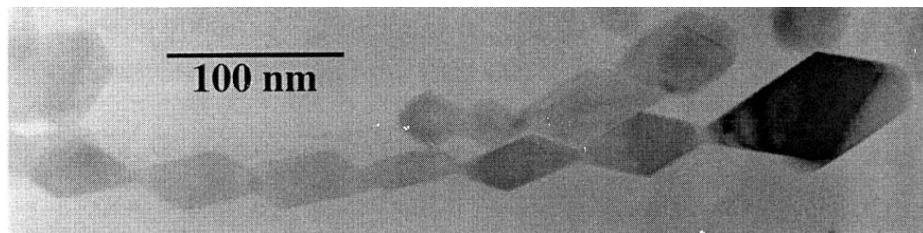
Nanocrystal growth in solution typically involves the fast nucleation of primary particles, followed by growth by:

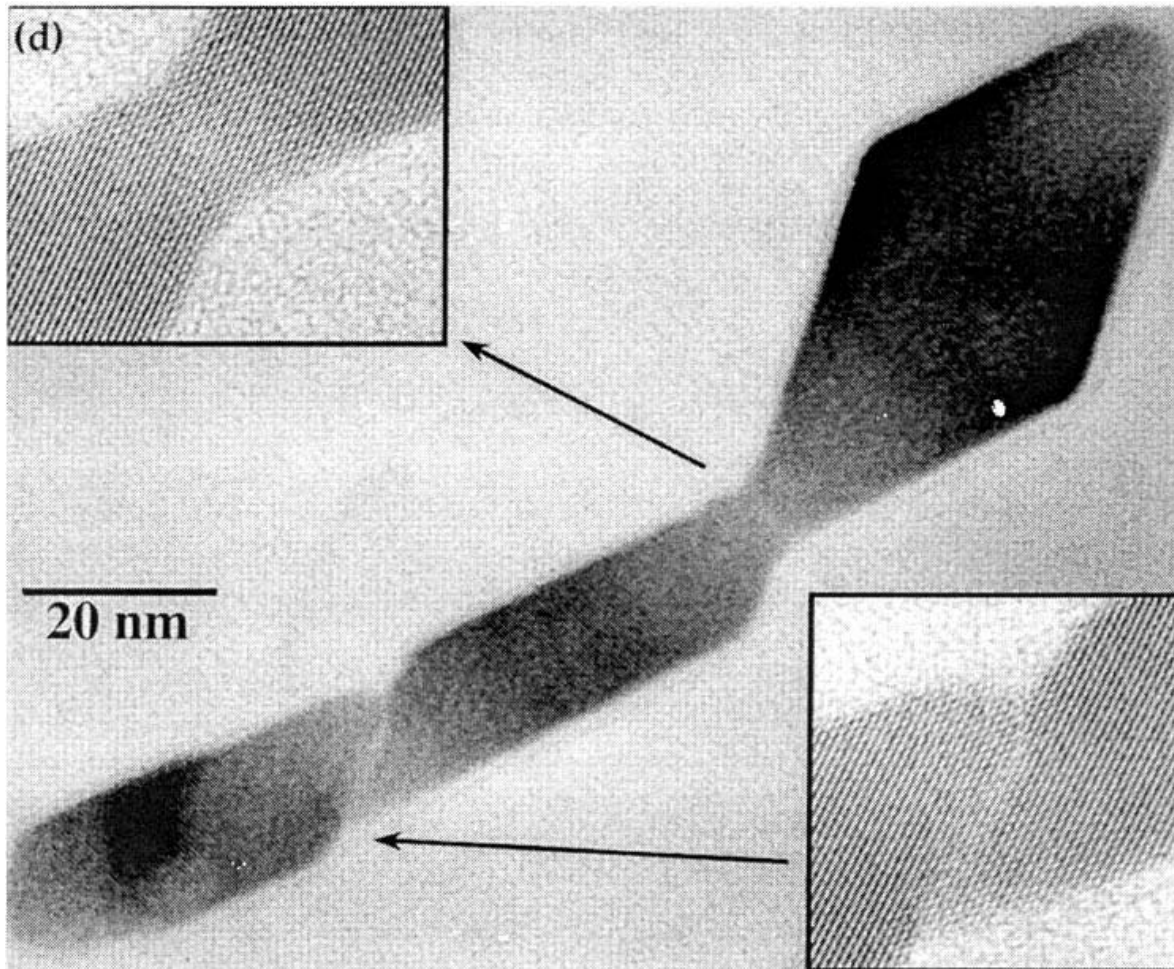
- **Coarsening**
- **Aggregation**



Oriented aggregation provides a special case

Nanocrystalline Titania Aggregates

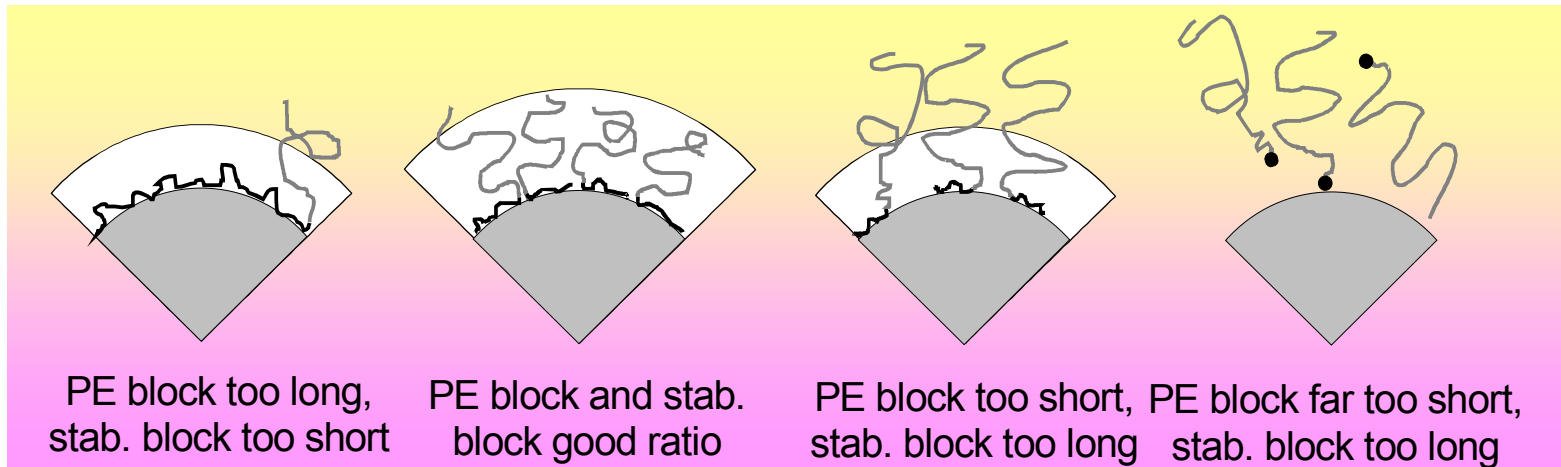




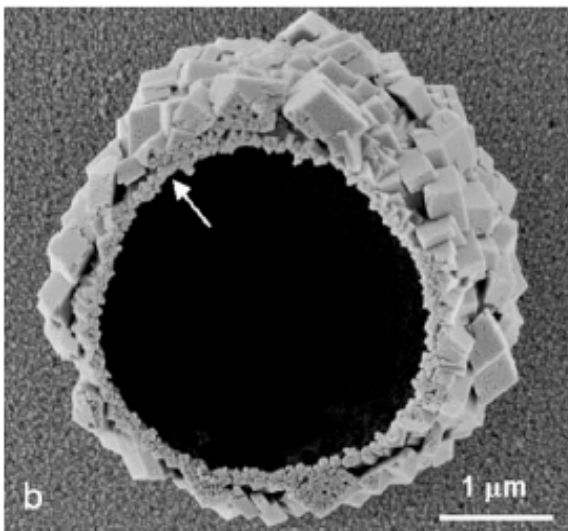
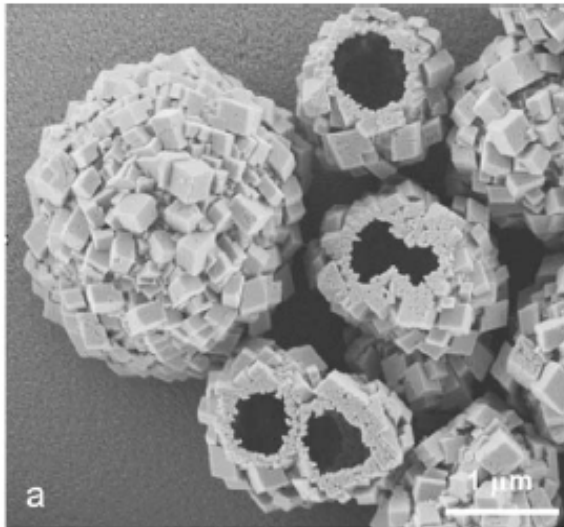
TiO₂ particles **aggregate** on **high energy faces** to produce elongated single crystals

Diblock Copolymers as Growth Additives

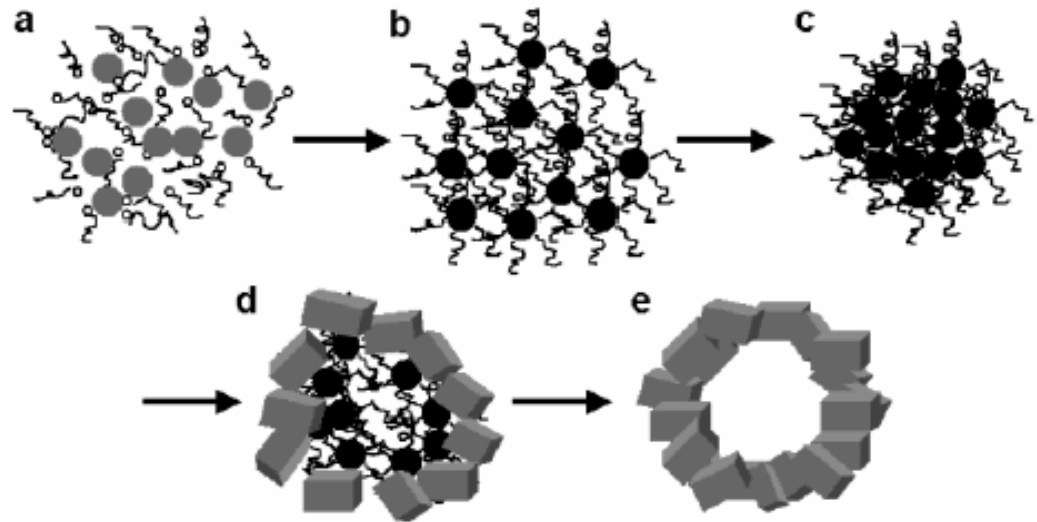
- Highly versatile in controlling crystal growth
- Used to produce homogeneous particle populations
- Particles of controlled morphologies
- Unusual highly-ordered polycrystalline structures
- Hierarchically ordered structures



CaCO₃ Hollow Spheres

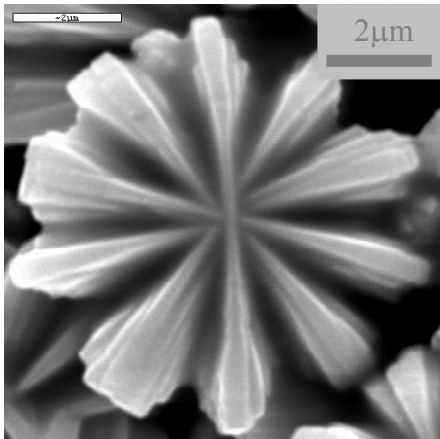


PEG-*b*-PMAA, ammonia diffusion

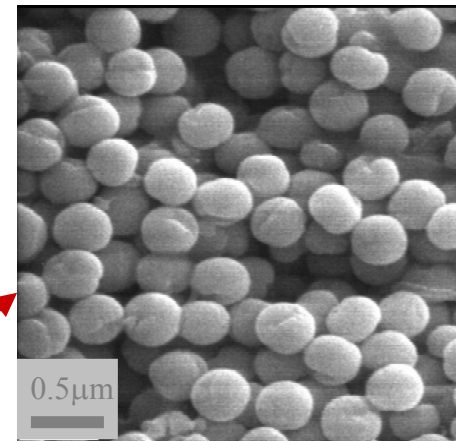


- Vaterite nanospheres aggregate
- Transformation to calcite starts on the surface - calcite rhombohedra form on particle surface
- Continue to grow at expense of dissolving vaterite

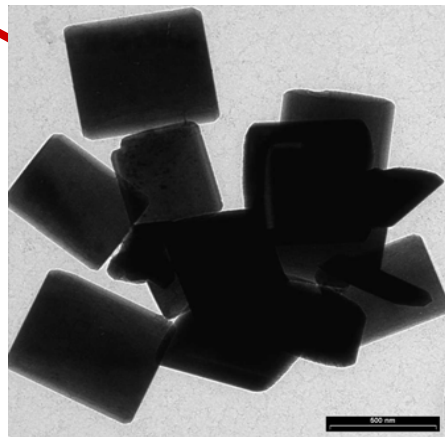
Control of BaSO₄ Precipitation



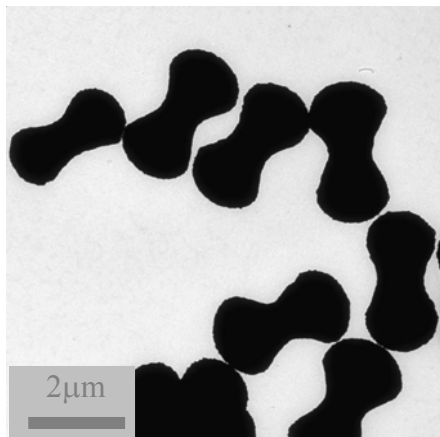
PEG-*b*-PEI-SO₃H



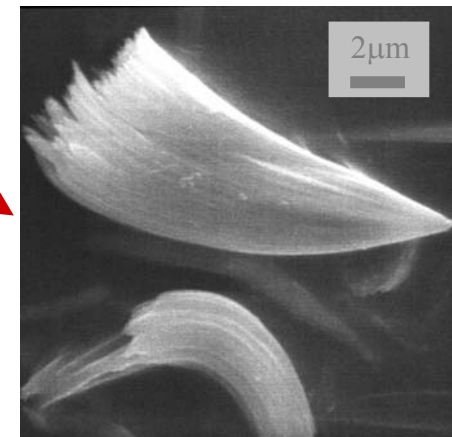
PEG-*b*-PMAA-Asp



No additive



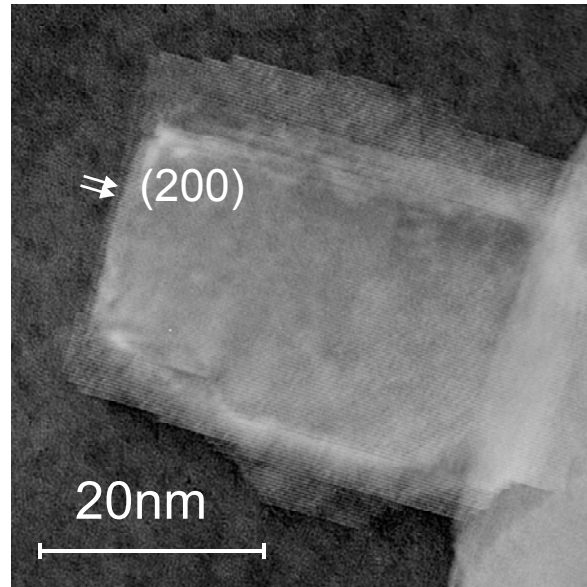
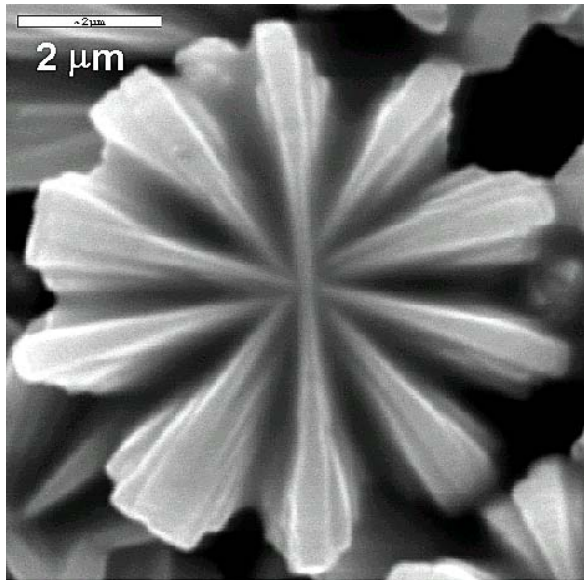
PEG-*b*-PEI-COOH



PEG-*b*-PMAA-PO₃H₂

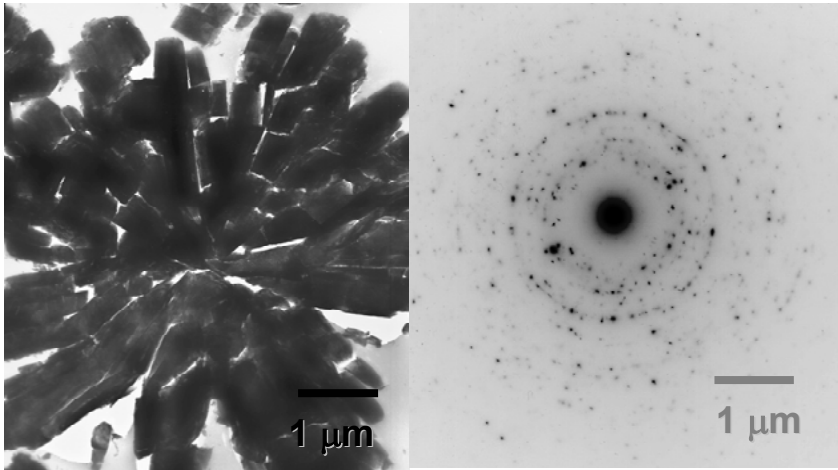
Formation of BaSO₄ "Flowers"

BaSO₄ with PEG-*b*-PEI-SO₃H additive, pH 5



- Flower-like structures with 10 petals
- Angles between petals almost equal
- Petals are overgrown
- Petals are single crystals with the same faces

Mechanism of Formation

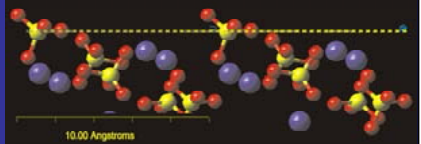
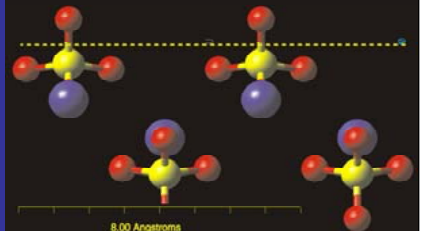
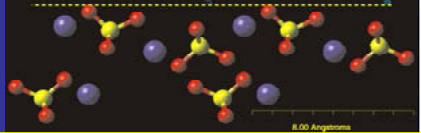
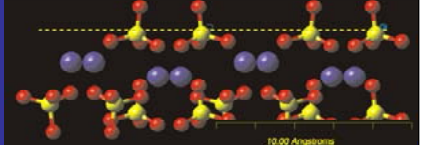
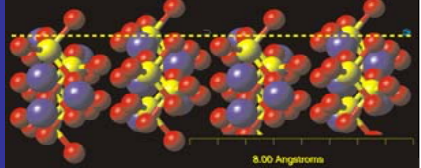
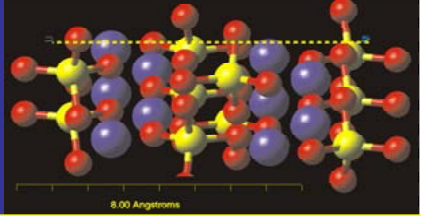


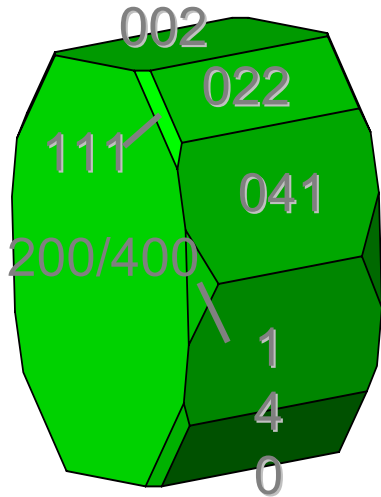
ED of thin section

⇒ (400) reflection much more intense than expected

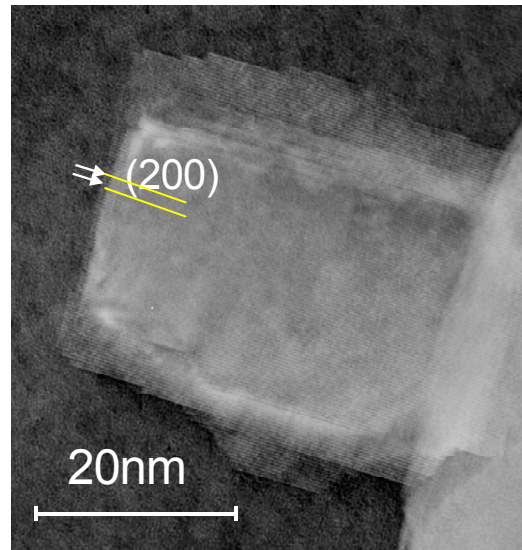
⇒ suggests possible exposed (200)/(400) faces

Polymer adsorption preferred on (200)/(400) faces

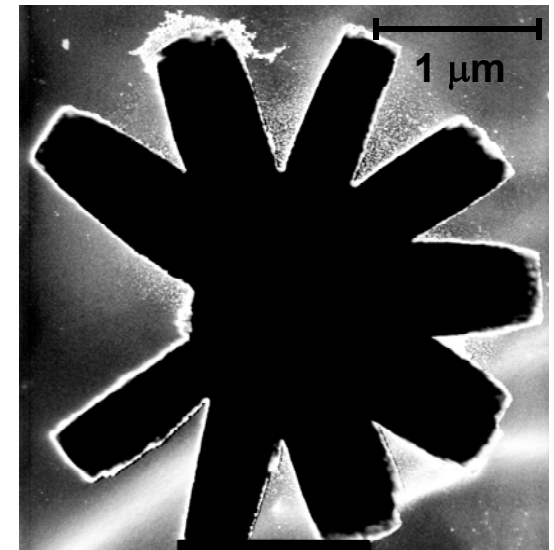
Ring	d (Å)	Plane	Atomar surface structure
1	3.852	111	
2	3.510	200	
3	2.772	002	
4	2.340	022	
5	2.170	140	
6	2.106	041	
7	1.769	400	As 200



Possible morphology of barite crystal



ED of single crystal "petal"
 ⇒ elongated along c-axis

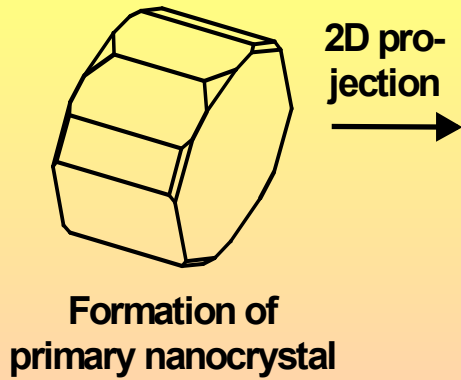


Dark field image constructed using (200) reflection

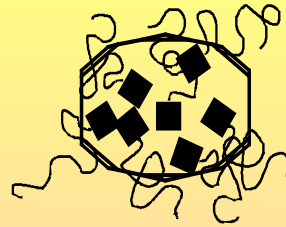
Petals do not grow epitaxially on underlying crystal

⇒ Dark field TEM

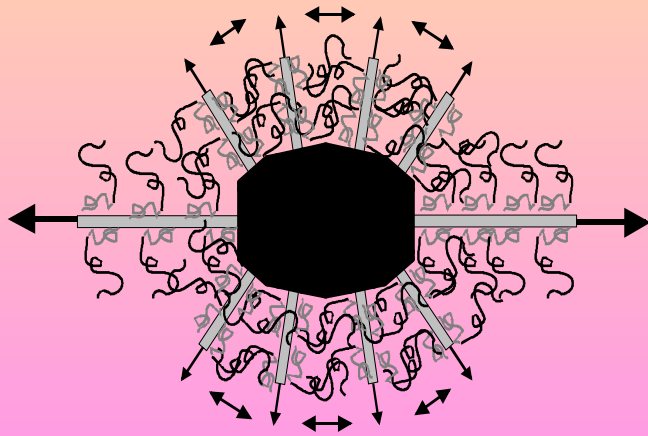
⇒ Equal separation of petals



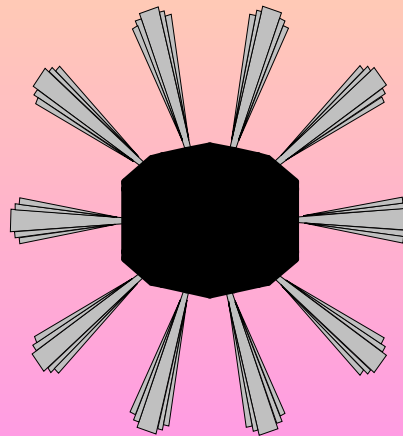
2D projection
→



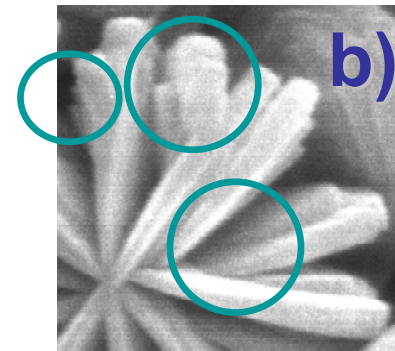
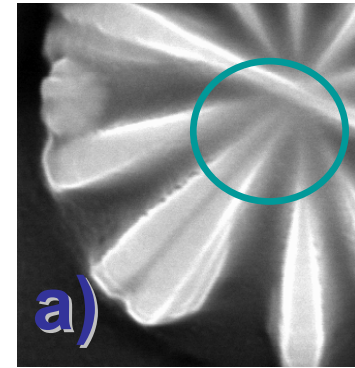
Polymers are adsorbed at 200/400 onto primary nanocrystal



Heterogeneous secondary growth at remaining 10 faces, Initial steric repulsion between petals, Reorientation to maximum distance



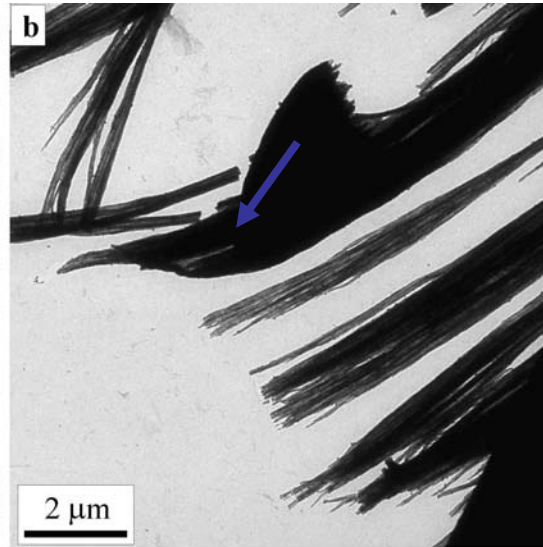
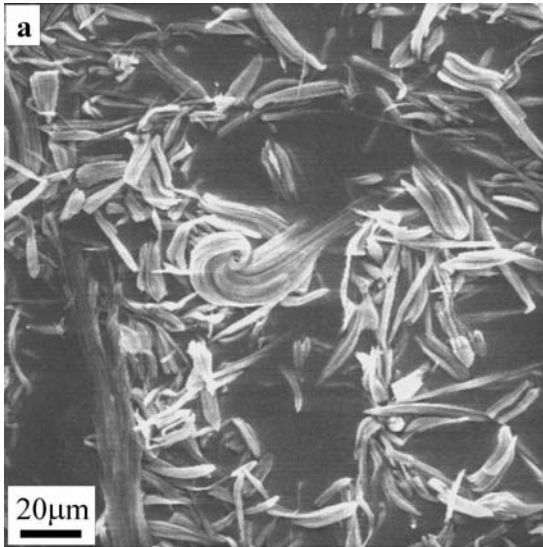
Overgrowth of petals



Observed defects:

- a) Nucleation of two petals on one side
- b) Crystallization at defects on petals

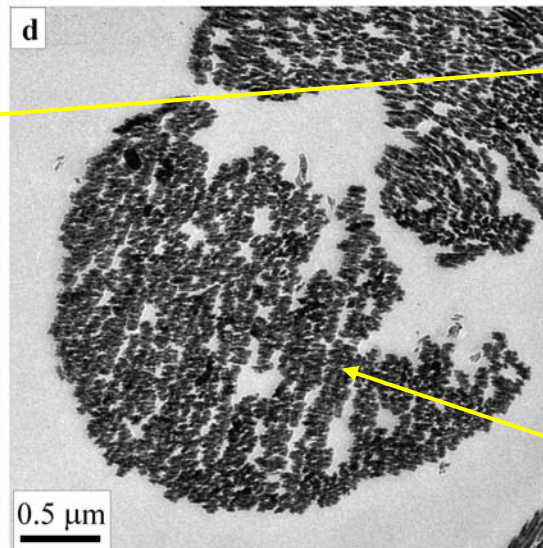
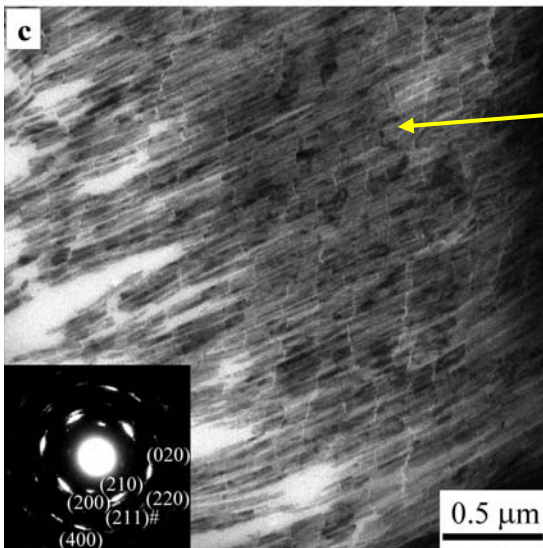
BaSO₄ Fibres



pH = 5

PEG-*b*-PMAA-PO₃H₂

Bundles of single crystalline fibers

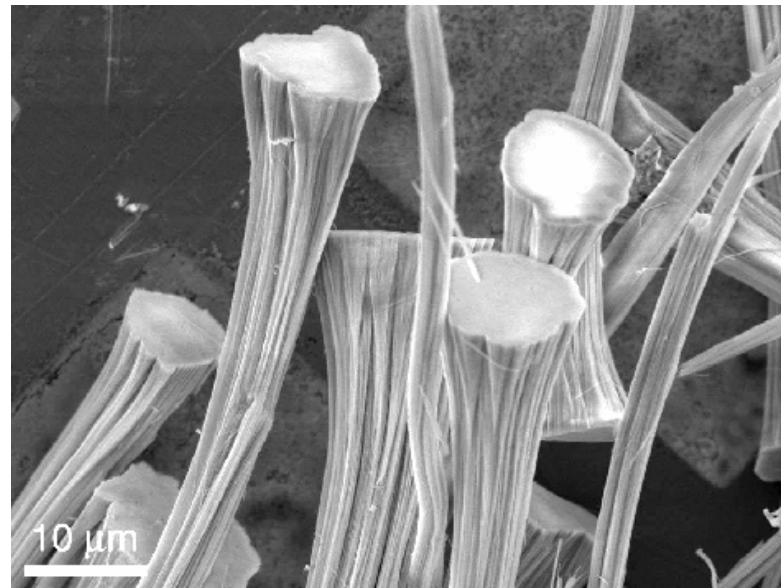
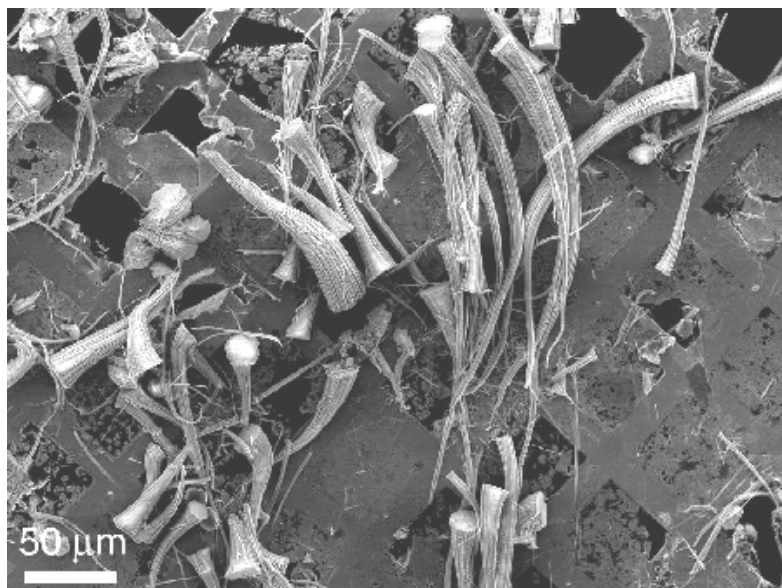


Parallel cut to fibre axis => [210]

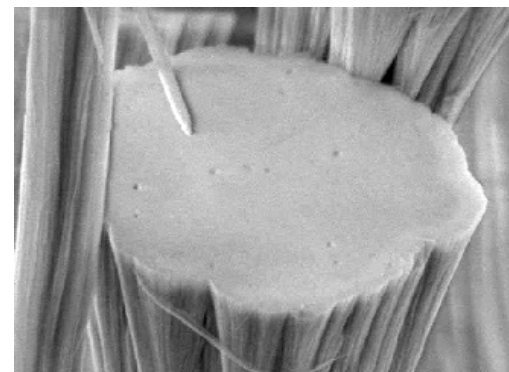
Perpendicular cut to fibre axis
Diameter 20 - 30 nm

BaSO₄ Fibers Obtained on Carbon Films

PEG-*b*-PMAA-PO₃H₂, 5 days, pH = 5

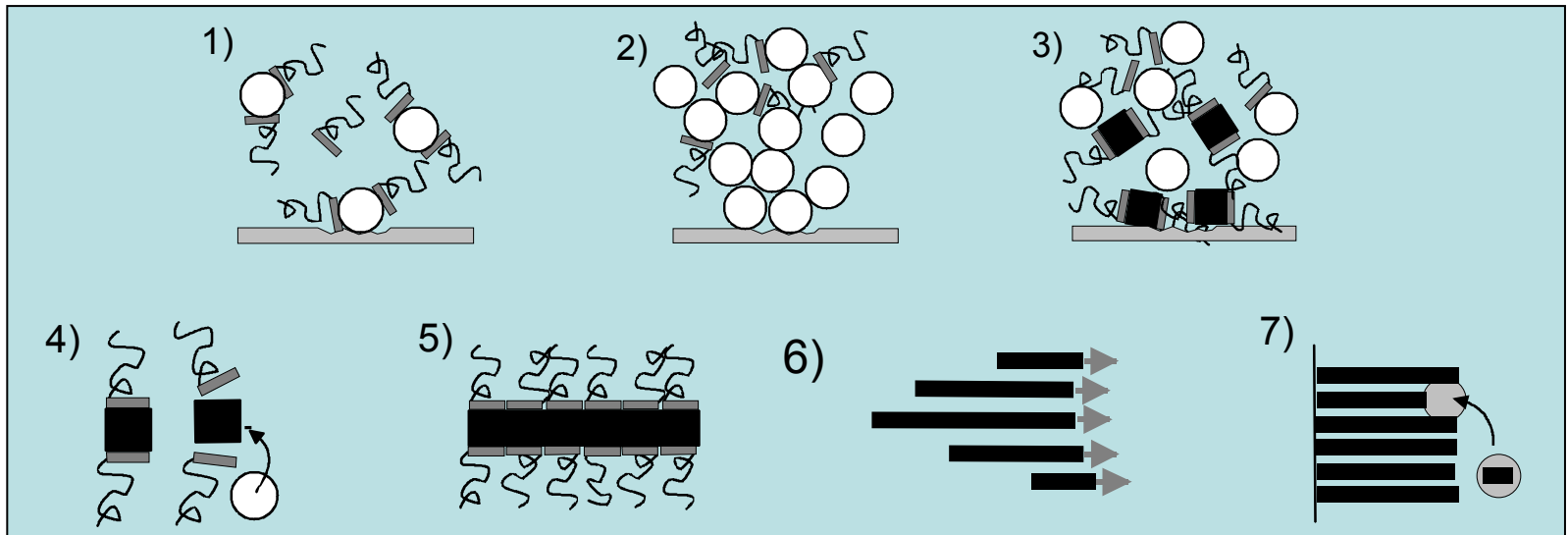
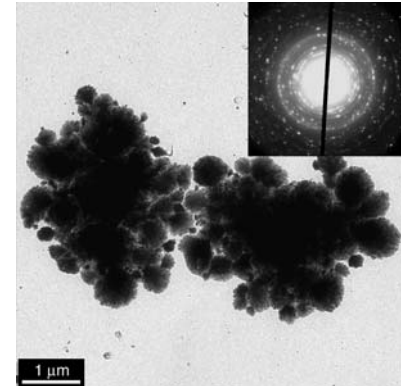
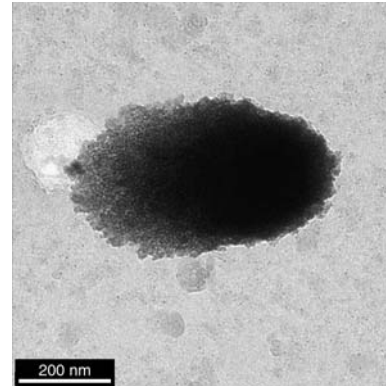


- Heterogeneous nucleation on carbon films
- Perfectly flat surface of growth edge



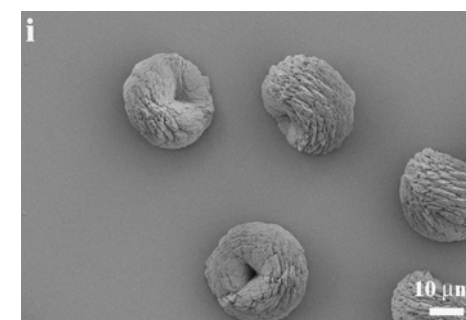
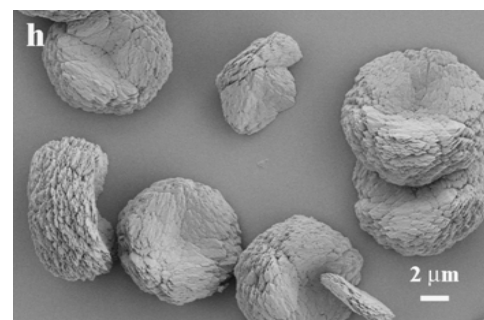
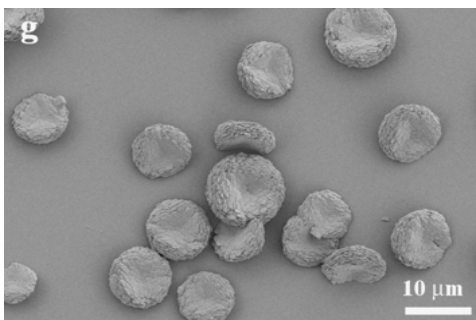
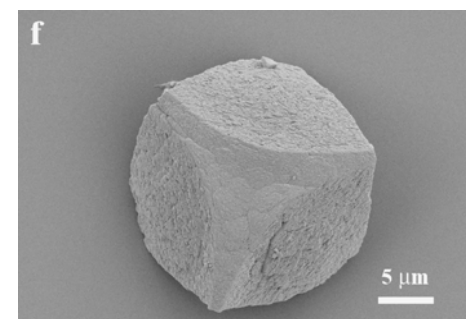
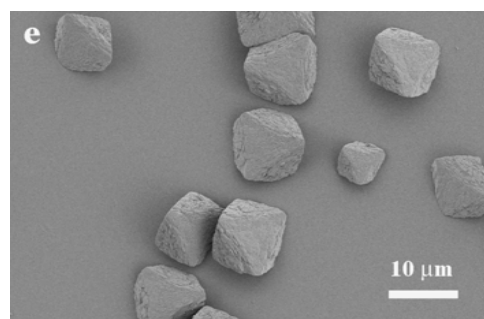
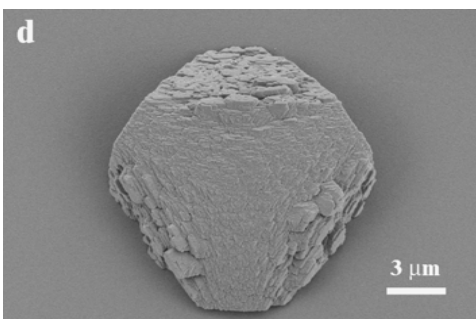
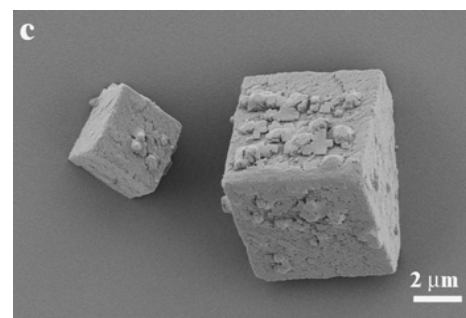
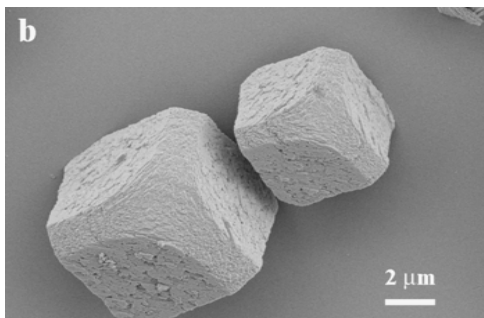
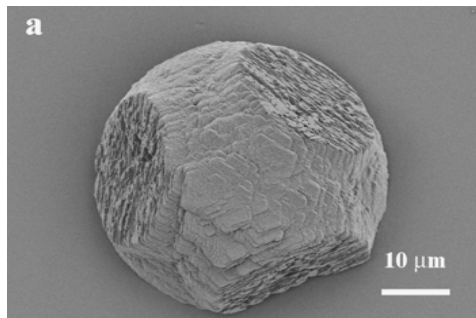
Mechanism of Fibre-Formation

- Form via amorphous BaSO_4 precursor particles
- Aggregate to form clusters \Rightarrow start to crystallise
- Anionic polymer chains adsorb to positively charged crystal faces



Different charges on different faces, and different shielding due to polymer adsorption may cause directional aggregation

CaCO₃ Mesocrystals



[Ca²⁺]
1.25 mM

[Ca²⁺]
2.5 mM

[Ca²⁺]
5.0 mM

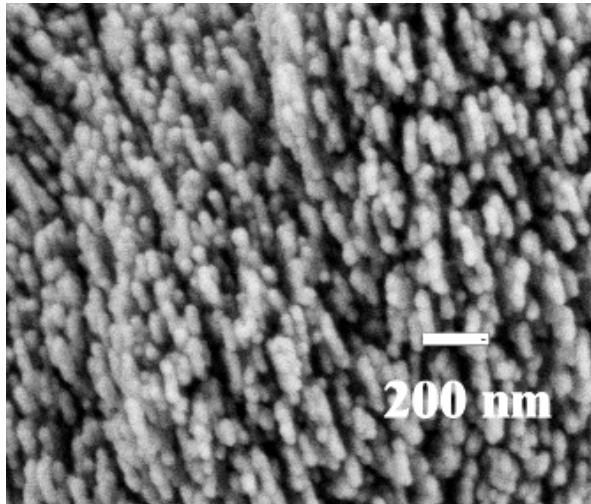
[PSS] = 1.0 g/L

[PSS] = 0.5 g/L

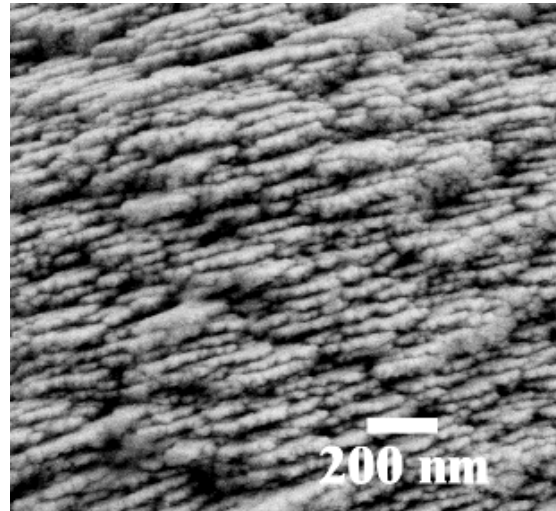
[PSS] = 0.1 g/L

Wang, Cölfen, Antonetti, *J. Am. Chem. Soc* (2005), 127, 3246-3247.

CaCO₃ Mesocrystals

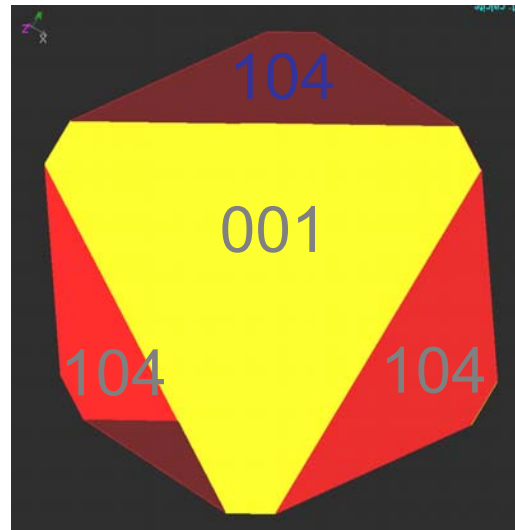
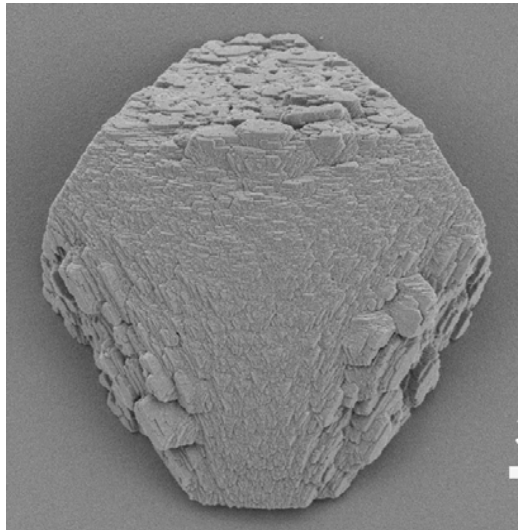


[PSS] = 1 g/L



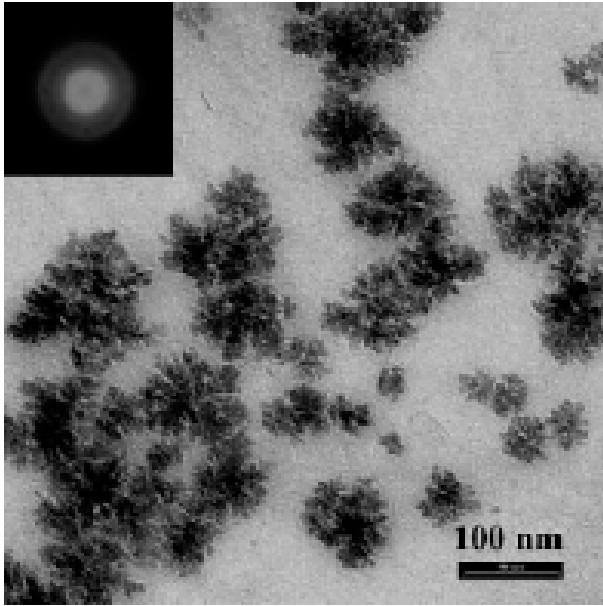
[PSS] = 0.1 g/L

[Ca²⁺] = 5 mM
7 hr



- Morphology like single crystal
- Extinguish under crossed polars as single crystal

Mechanism



- Amorphous CaCO_3 precursor particles

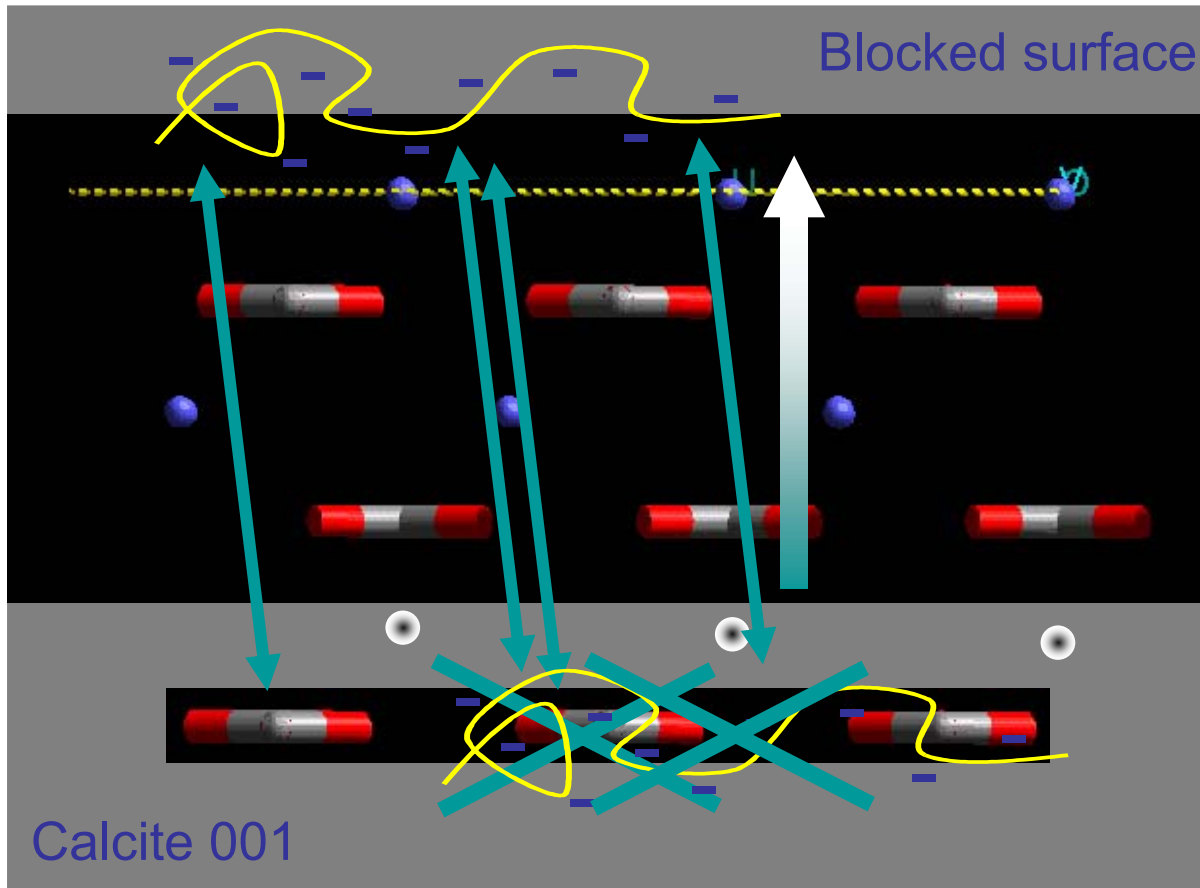
- ACC particles aggregate and crystallise

- Crystal units assemble to form "mesocrystals"

- PSS is selectively adsorbed on positive (001) faces of nanocrystals

- Adsorption of negative species to opposite surface is prevented by dielectric interaction throughout the crystal

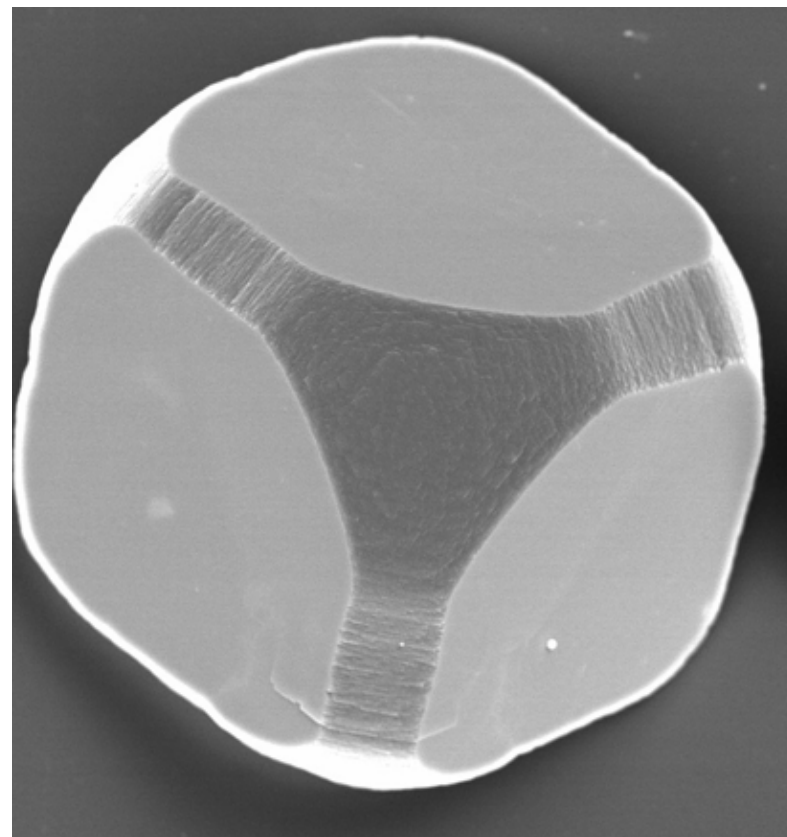
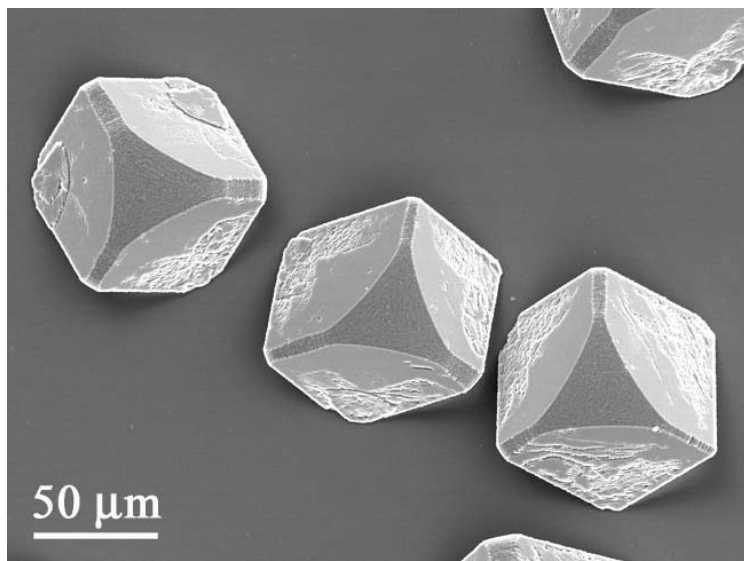
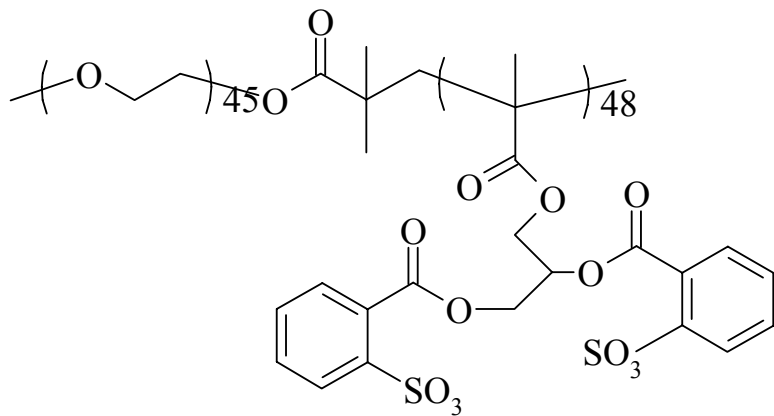
- Resulting dipole along the *c*-axis drives nanoparticle assembly



A dipole is induced in the very thin platelets which have exposed (001) faces

⇒ Two oppositely charged faces produced, which drives aggregation

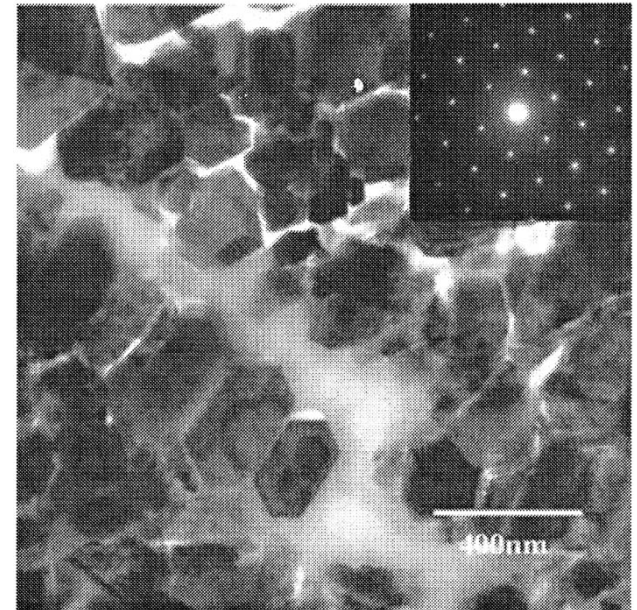
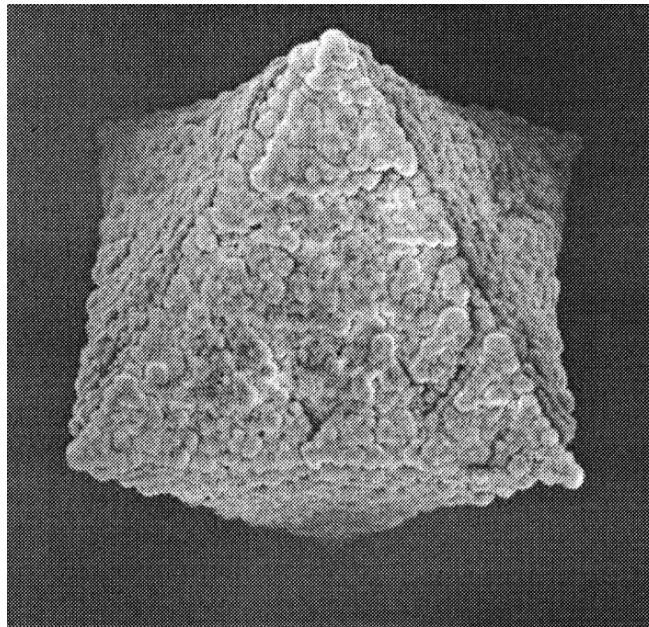
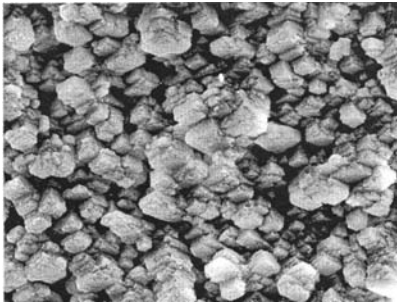
Sulphonate Functionalised Copolymers



Gel-Grown Calcite Aggregates

Calcite crystals grown in pol-acrylamide hydrogels using double diffusion \Rightarrow Remarkable **crystal aggregates** formed

Pseudo
octahedral
morphology

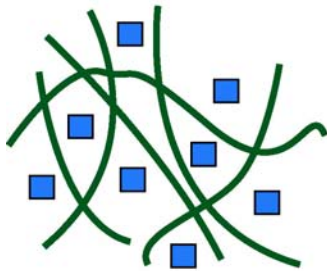


Diffraction shows entire aggregate behaves as a single crystal !

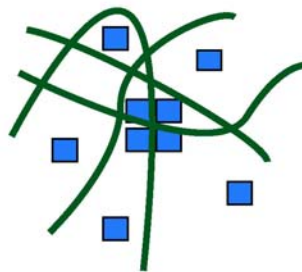
Grassman et al, *Am. Mineral.* 2003, 88, 647-652.

Mechanism

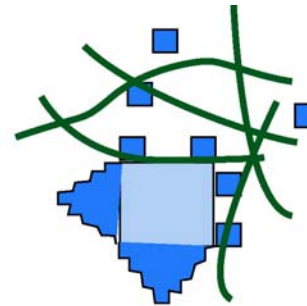
- **Supersaturation** is high in the gel \Rightarrow nucleation burst occurs
- Some nuclei grow by adsorption of ions to reach a supercritical size
- Further growth can then occur by adsorption of clusters to the large faces of the particle \Rightarrow **reduces the surface energy of the face**



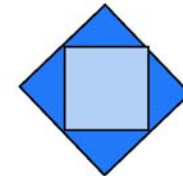
Homogeneous
Nucleation



Critical
Nucleus



Heterogeneous
Cluster
Nucleation



Product
Octahedral
Shape

\Rightarrow **Pseudo-octahedral morphology results**

Templating Routes to Nanoparticles

Many examples:

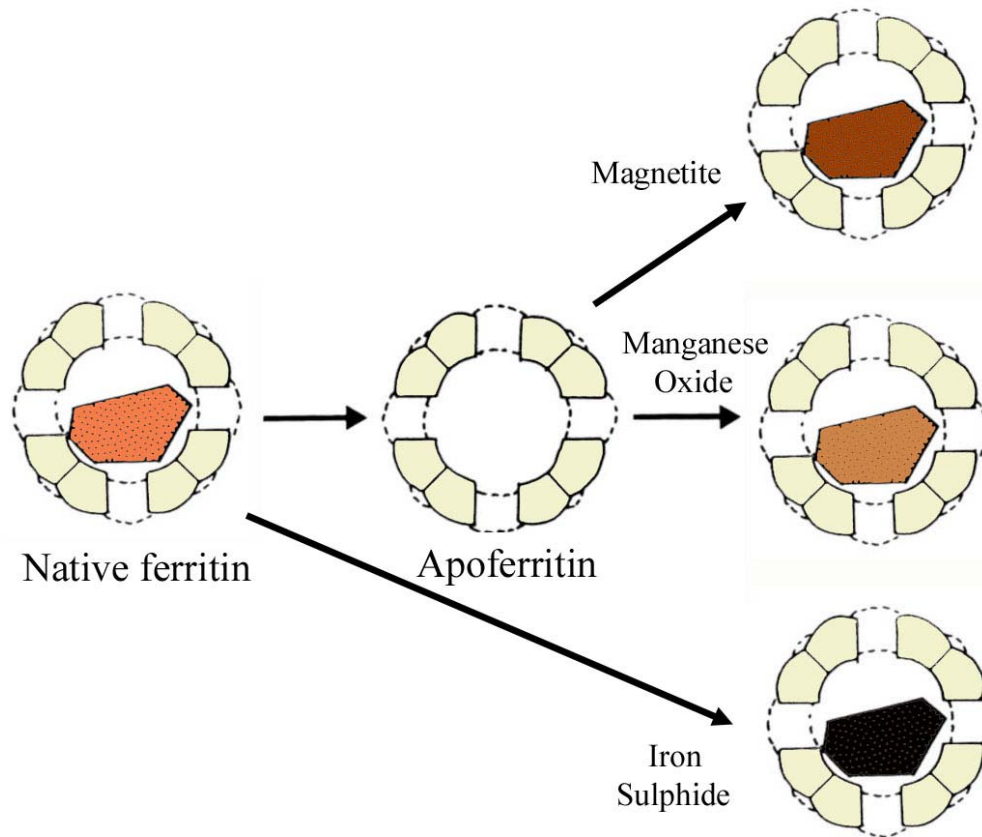
- Crystallisation in micelles
- Crystallisation in vesicles
- Polymer capsules

Look at two examples profiting from biological structures:

- Crystallisation in ferritin
- Crystallisation in viruses

Synthesis of Nanoparticles within Ferritin

Ferritin is a uniquely stable protein \Rightarrow can be used as a reaction vessel in which to synthesise a range of inorganic particles



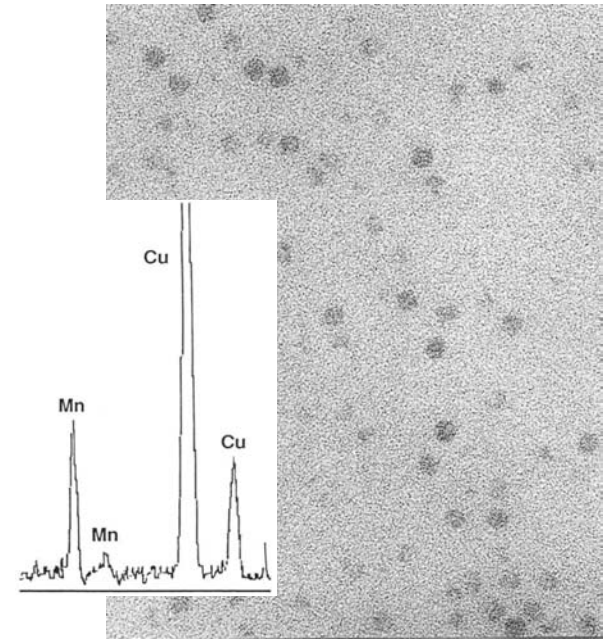
Meldrum, Wade, Nimmo, Heywood, Mann (1991) *Nature* 349, 684-687.

Formation of MnOOH Cores

Reconstitution of apoferritin with Mn(II)

⇒ alternative redox active metal

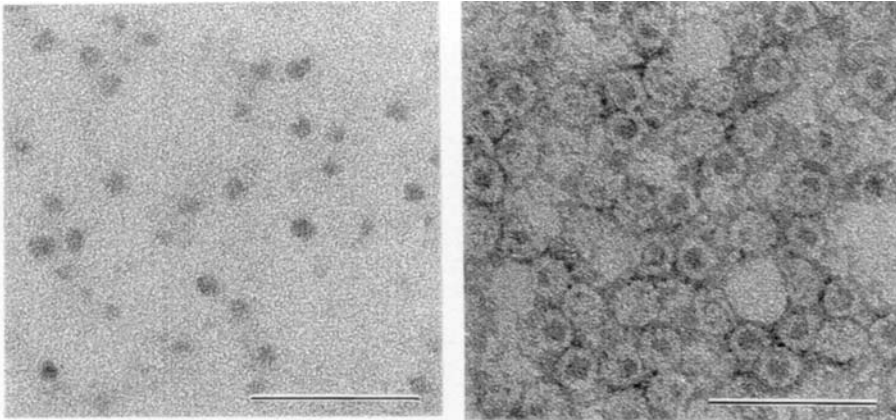
pH 8.9 - poorly ordered Mn oxide core formed over weeks



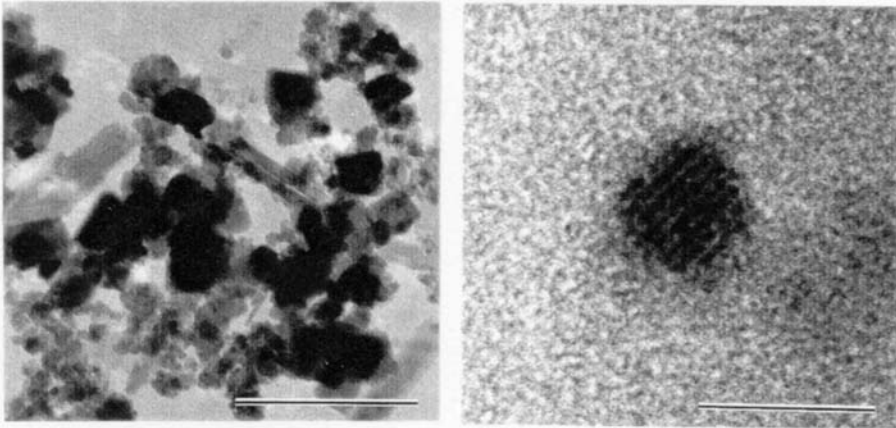
- Significantly more non-specific precipitation than in Fe(II) reconstitutions
- Cores always large, but only present in a proportion of ferritin molecules.
- Ferritin provides a nucleation site for MnOOH, but shows poor catalytic activity towards the oxidation of Mn(II)

Magnetite - "Magnetoferritin"

Modify reconstitution conditions with Fe(II) \Rightarrow magnetite



- pH 8.5
- slow oxidation
- 60°C



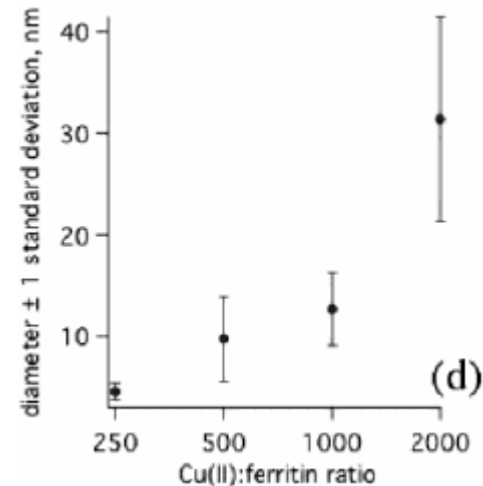
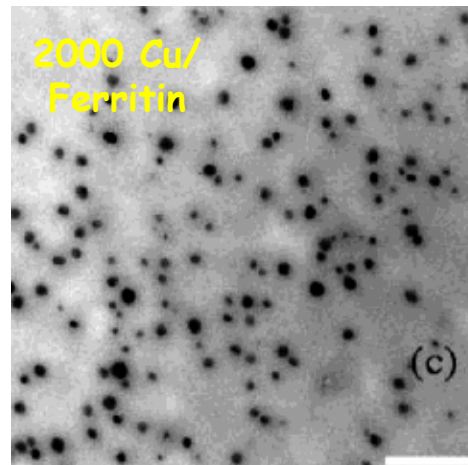
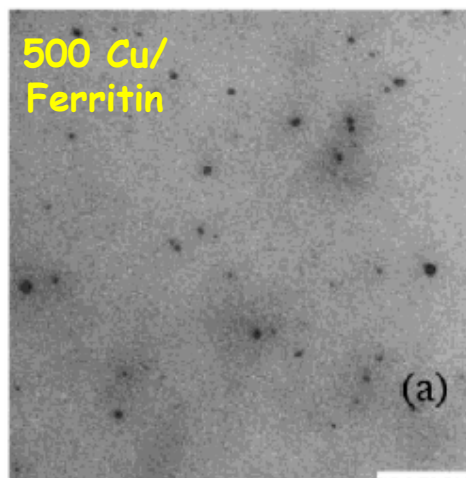
\Rightarrow Magnetite rather than ferrihydrite

Photocatalytic Synthesis of Copper Colloids in Ferritin

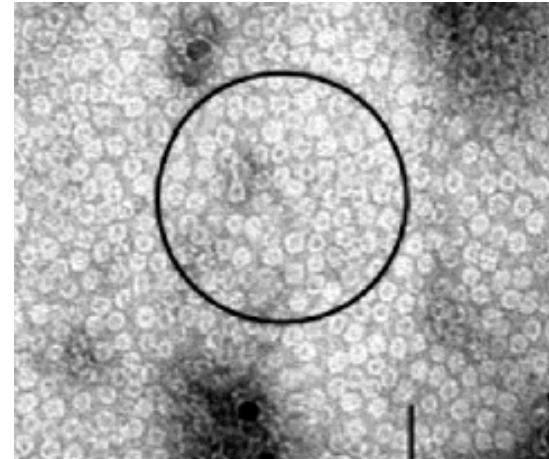
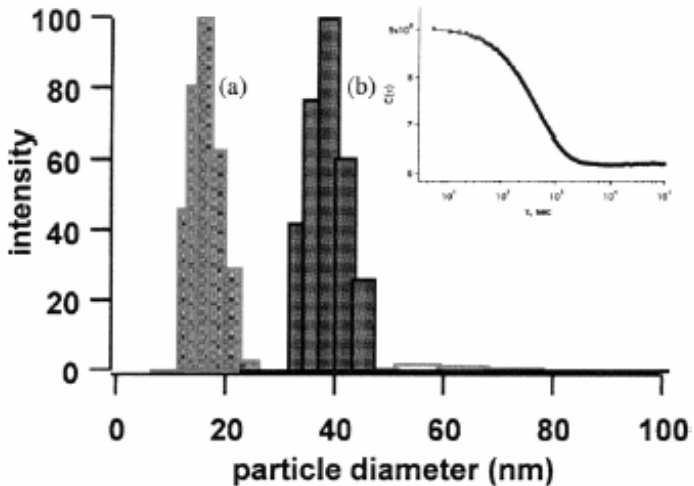
Mineralised ferritin can act as a photocatalyst for redox reactions

⇒ Ferrihydrite core may act a **visible-band-gap semiconductor**

Form **Cu nanoparticles** on photocatalytic reduction of **Cu(II)** in the presence of mineralised ferritin in the presence of a sacrificial reductant (citrate)



Mechanism



DLS indicates **DISCRETE** particles, sizes 36nm for 2000-Cu, 28nm for 1000-Cu and 16nm for 500-Cu

⇒ All **LARGER** than protein shell ⇒ **DISRUPTION**

⇒ Images suggest particles formed within protein shell



Slow nucleation is followed by fast growth

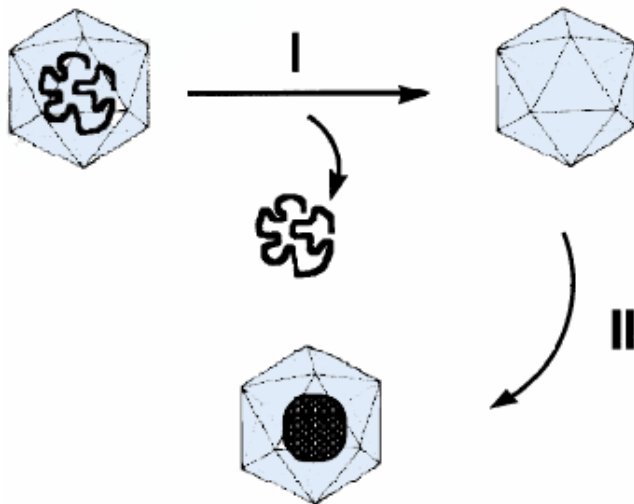
Nanoparticle Synthesis in Virus Protein Cages

Viruses act as host containers for nucleic acid storage and transport

Occur in **wide range of sizes and morphologies**

⇒ offer more versatile “protein reaction vessel” than ferritin

⇒ use virus cage in **formation and entrapment** of inorganic and organic polymer species

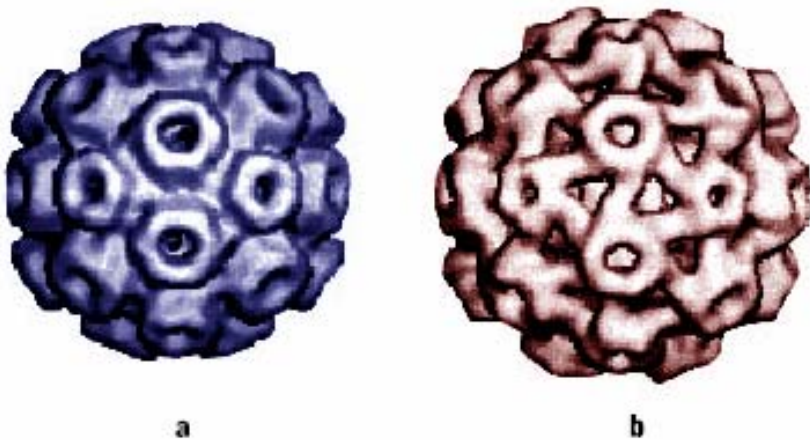


I Removal of viral RNA and purification of the empty virus particle

II Selective mineralization within the confines of the virus particle

Synthesis of Paratungstate Particles in Cowpea Chlorotic Mottle Virus (CCMV)

Many virions undergo **reversible structural changes**, that open up **pores in the structure**, giving access to the cage interior



CCMV in
(a) Unswollen condition at low pH
(b) Swollen condition at high pH.

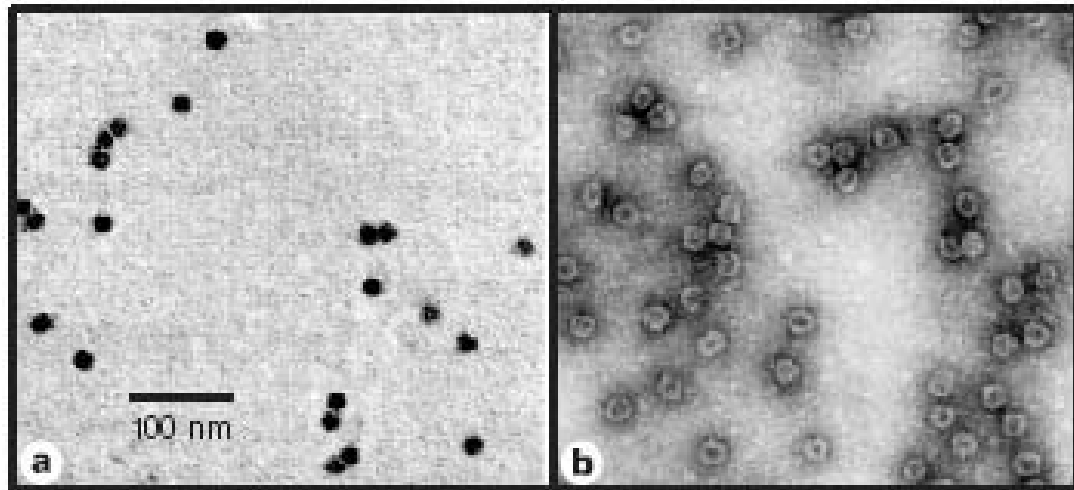
Swelling causes formation of 60, 2nm pores

- CCMV \Rightarrow 28 nm outer, 18 nm inner diameter
- Positively charged interior/ outer surface not highly charged
- Inner surface provides unique chemical environment
- CCMV - Swells pH > 6.5, reverses pH < 6.5

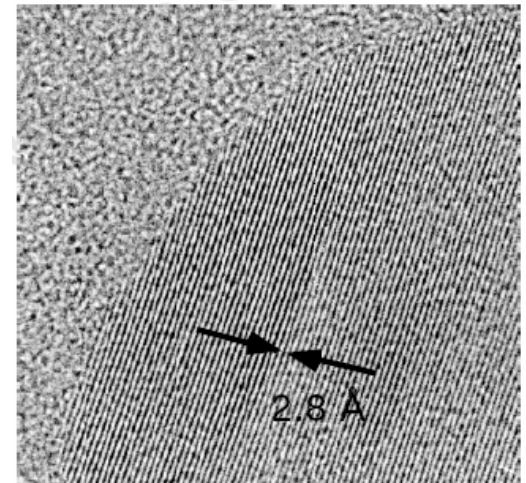
Douglas and Young, *Nature*, 1998, 393, 152-154.

Paratungstate particles ($\text{H}_2\text{W}_{12}\text{O}_{42}^{10-}$) formed in virus host cage

- Aqueous molecular tungstate (WO_4^{2-}) species incubated with virus cage > pH 6.5
- Polymerisation induced by reduction in pH < 6.5

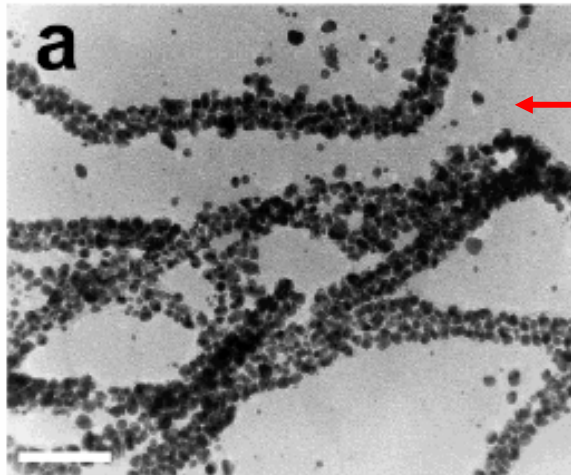


TEM images of paratungstate-mineralized virus particles (a) unstained (b) negatively stained

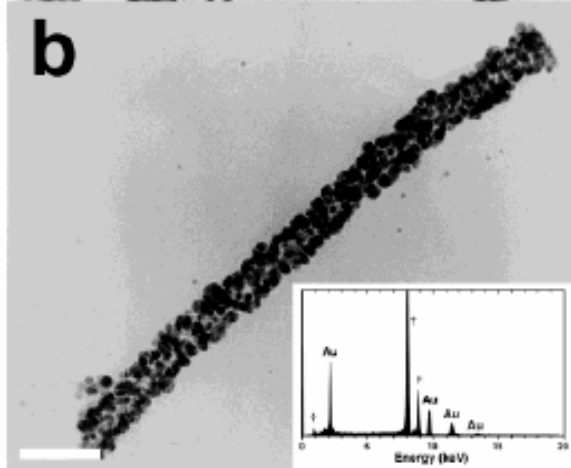


HRTEM image of part of a paratungstate core

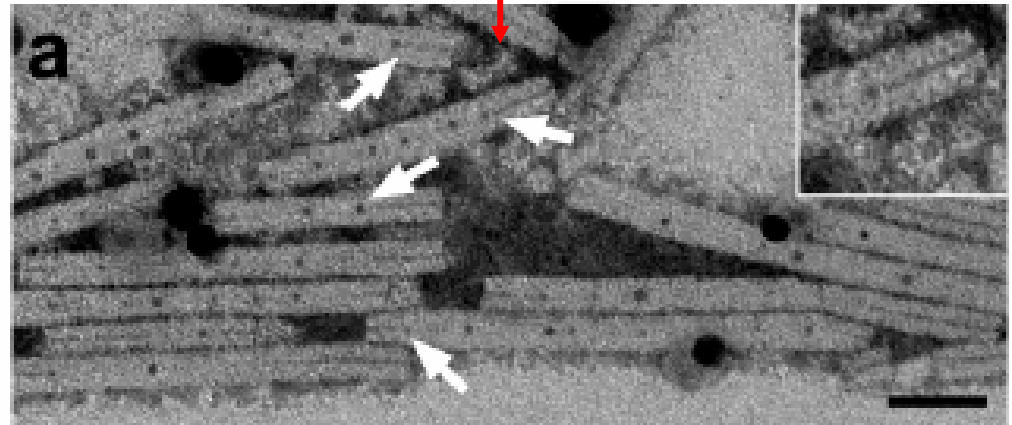
Organization of Metallic Nanoparticles using Tobacco Mosaic Virus



External surfaces of TMV rods decorated with metal nanoparticles on chemical reduction of $[PtCl_6]^{2-}$ or $[AuCl_4]^-$ at low pH



Photochemical reduction of Ag(I) salts at pH 7 resulted in nucleation of Ag nanoparticles within the internal channel

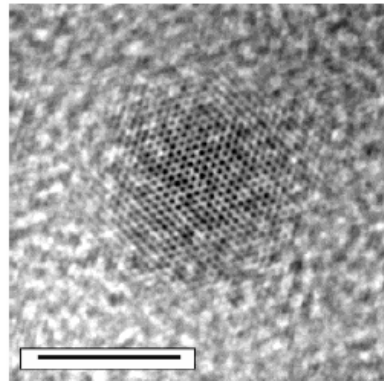
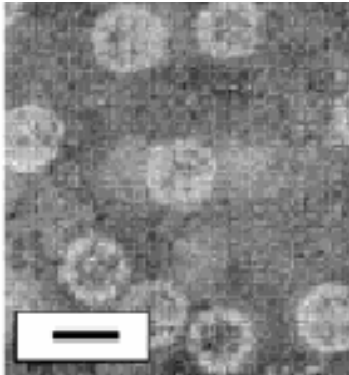


Protein Engineering of Viral Cage

CCMV offers cationic cage interior \Rightarrow alter to provide a more versatile reaction vessel

CCMV protein coat genetically modified by replacing 9 basic residues at N-terminus with glutamic acid

\Rightarrow Does not affect assembly, and interior surface becomes anionic



Iron oxide particles formed in modified CCMV protein shells

\Rightarrow Lepidocrocite (γ -FeOOH)

Mechanism

- Lepidocrocite (γ -FeOOH) formed - same as in control reactions

- Negatively charged interior accumulate Fe(II) ions

⇒ Aggregation may change the redox potential of Fe(II)

⇒ Interior surface acts as a nucleation site by clustering Fe(II)/Fe(II) ions at the interface

- After nucleation, the initially formed crystallite can act as a catalytic site for further oxidative hydrolysis

Can form up to 24 nm cores - upper limit of virus cage

Templating Polycrystalline Structures

Large complex structures \Rightarrow currently cannot be produced via self-assembly techniques

Alternative method \Rightarrow Templating

Soft templates

eg microemulsions

Rigid organic templates

eg. pollen grains

Inorganic templates

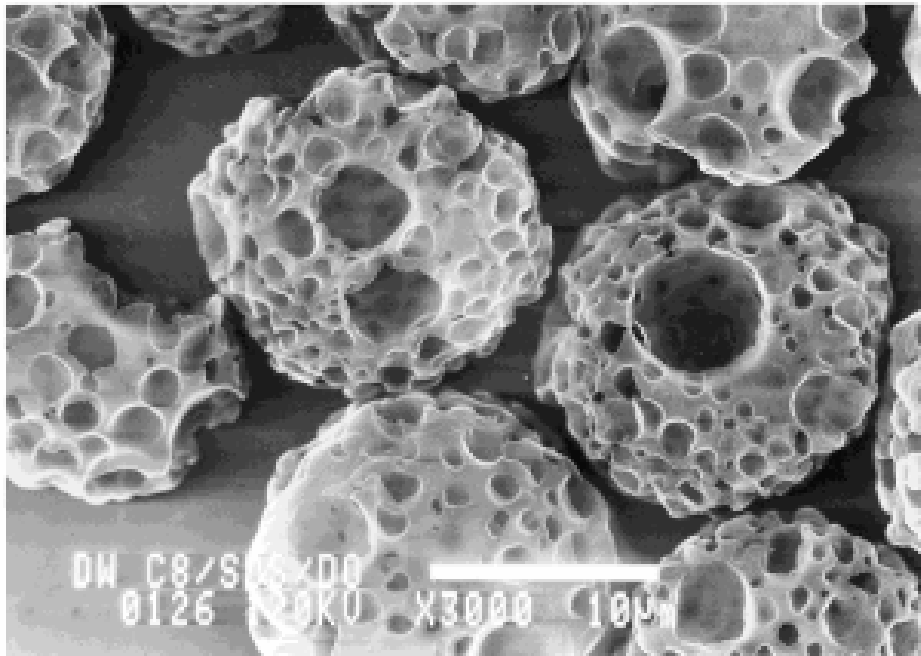
eg. sea urchin skeletal plates

eg diatoms

Templating Microemulsions

Spherical vaterite particles with sponge-like microstructures

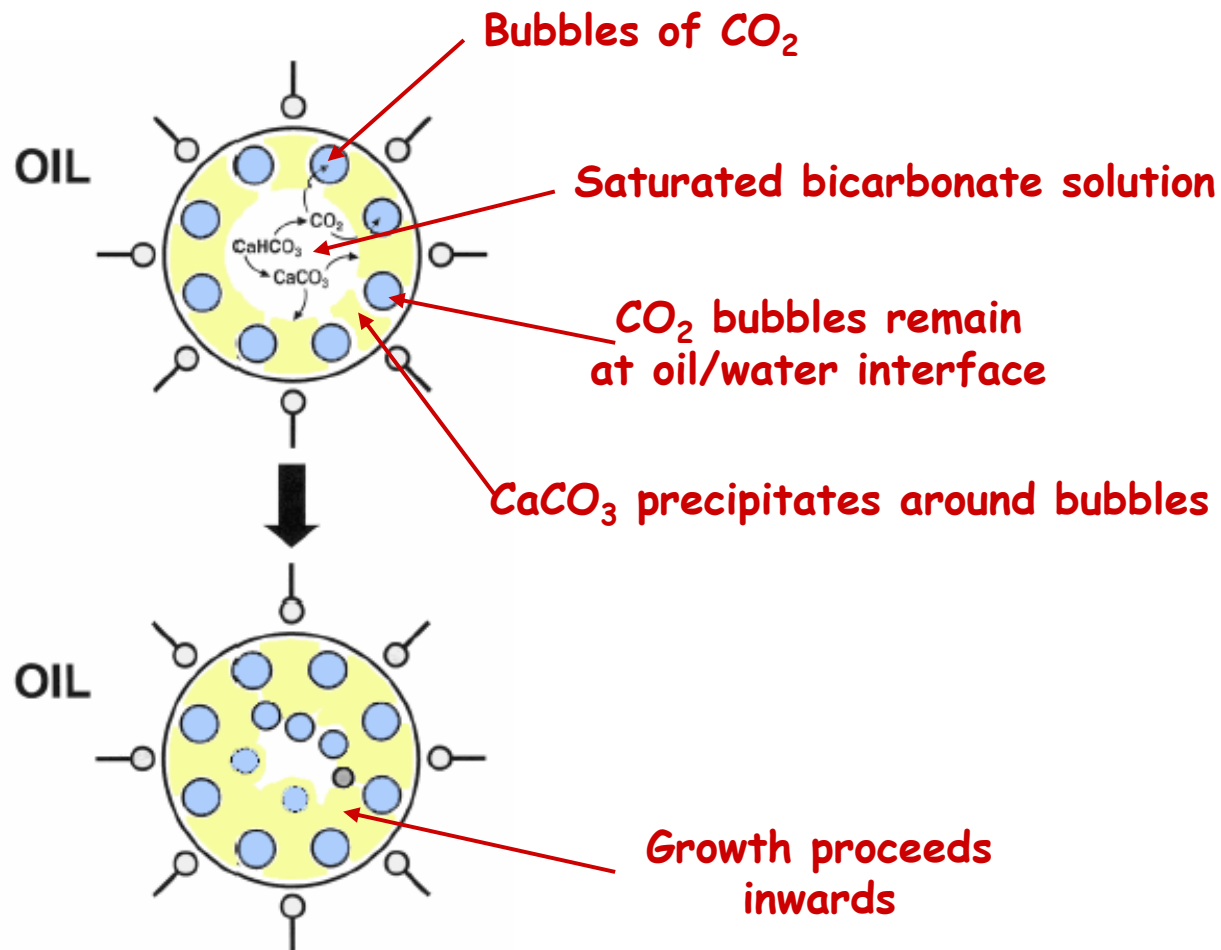
⇒ Produced by evaporation of SDS/octane/supersaturated calcium bicarbonate solution water-in-oil microemulsions



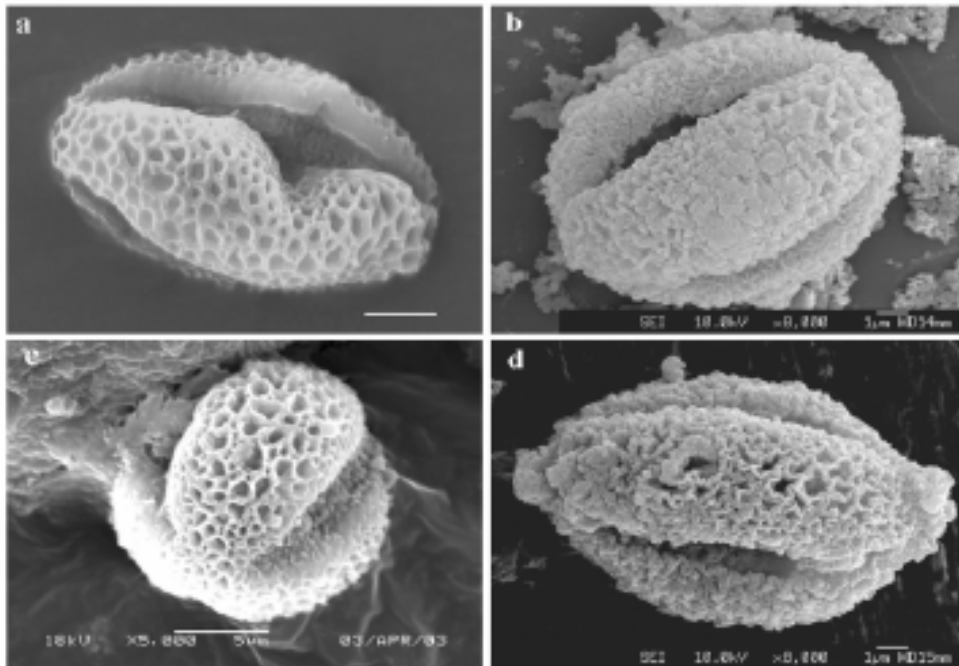
- Typically show irregular surface depressions and pores

- Many highly porous with a perforated outer shell and a partially hollow centre,

- Micro-emulsion solution contains micron-sized water droplets
- Mineral aggregates initially form along the surface of water droplets \Rightarrow form perforated hollow shells with smooth surfaces

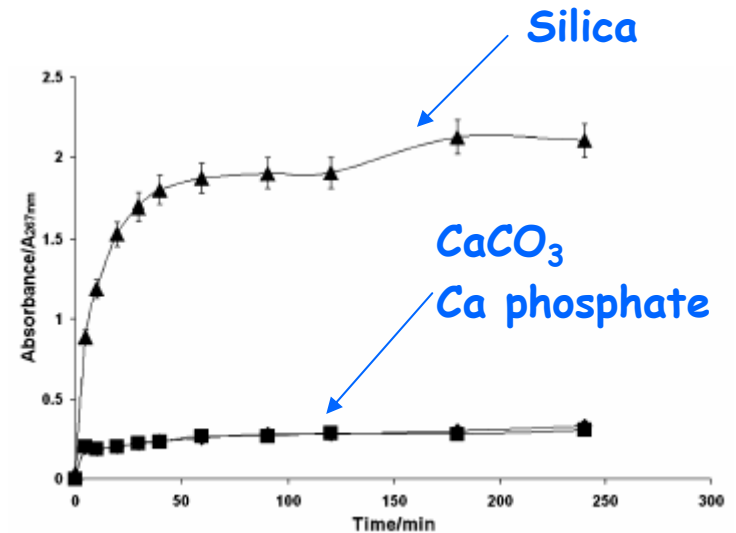


Complex Morphologies using Pollen Grain Templates



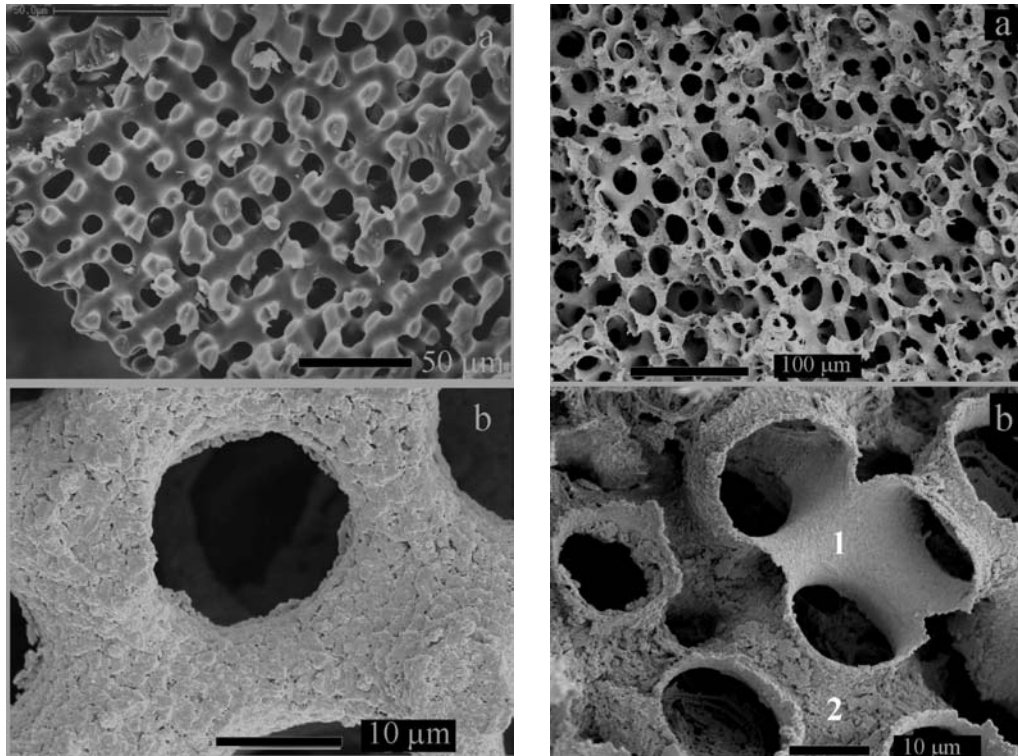
- (a) Uncoated pollen grain
- (b) Calcium phosphate
- (c) Calcium carbonate
- (d) Silica

Replicas investigated for drug release
⇒ release of ibuprofen



Templating Sea Urchin Skeletal Plates

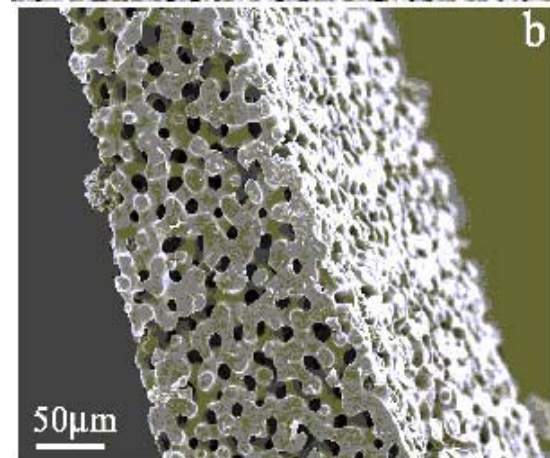
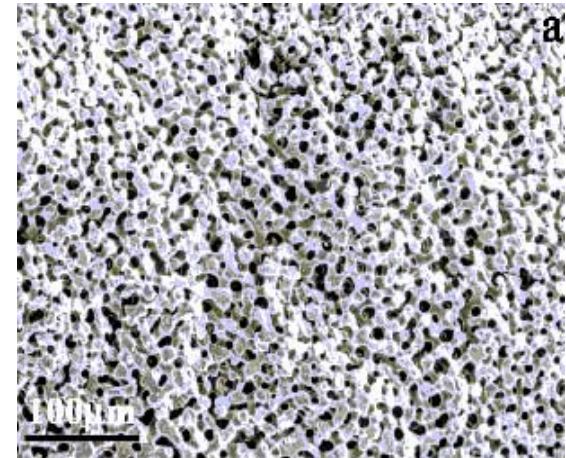
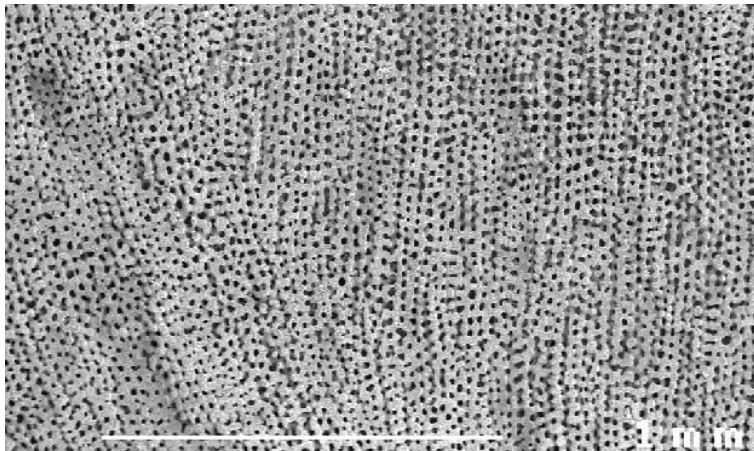
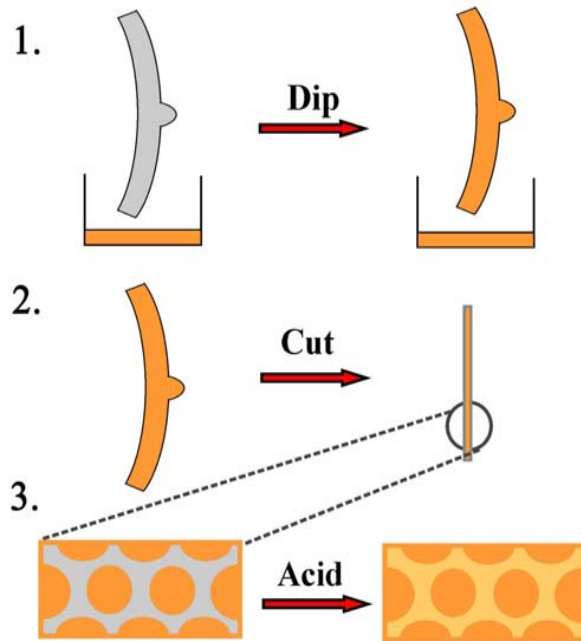
Sea urchin plates have a remarkable morphology - use as template for synthesis **macroporous solids**



- Urchin plate dipped in a solution of stabilised gold particles
- Annealed • CaCO_3 dissolved \Rightarrow **POROUS GOLD**

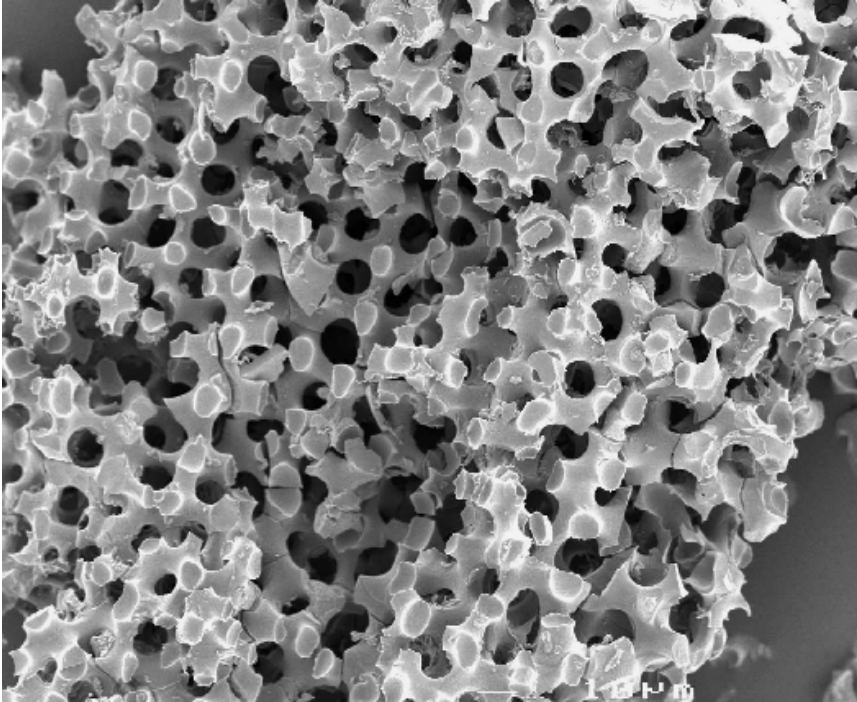
Meldrum F.C., Seshadri R. *Chem. Comm.* (2000) 29-30.

Polymer Replica

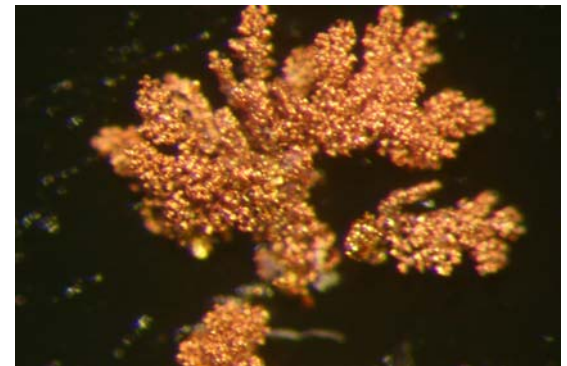
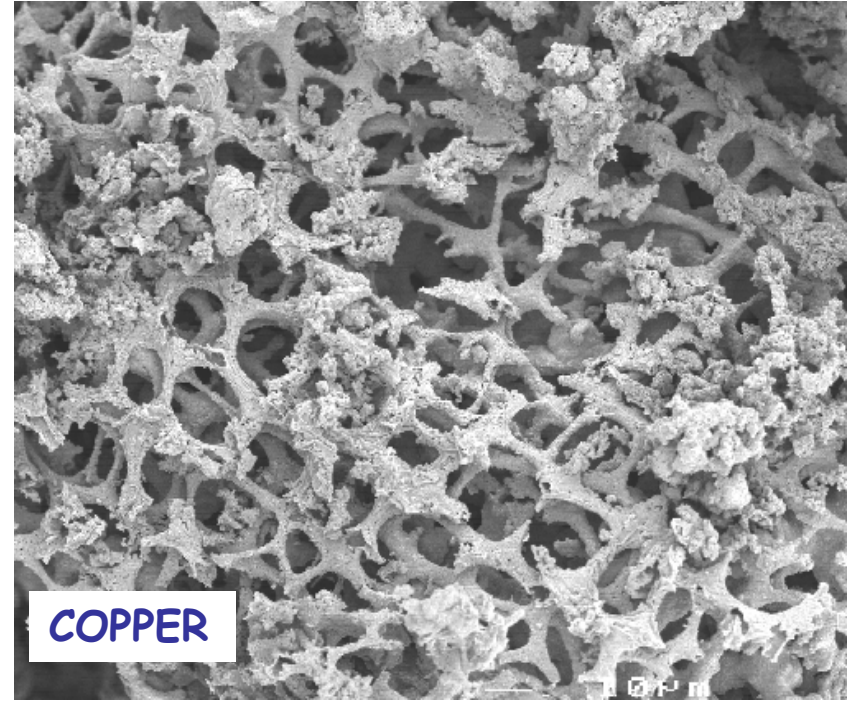


Polymer template is readily dissolved in chloroform

Templating of TiO₂



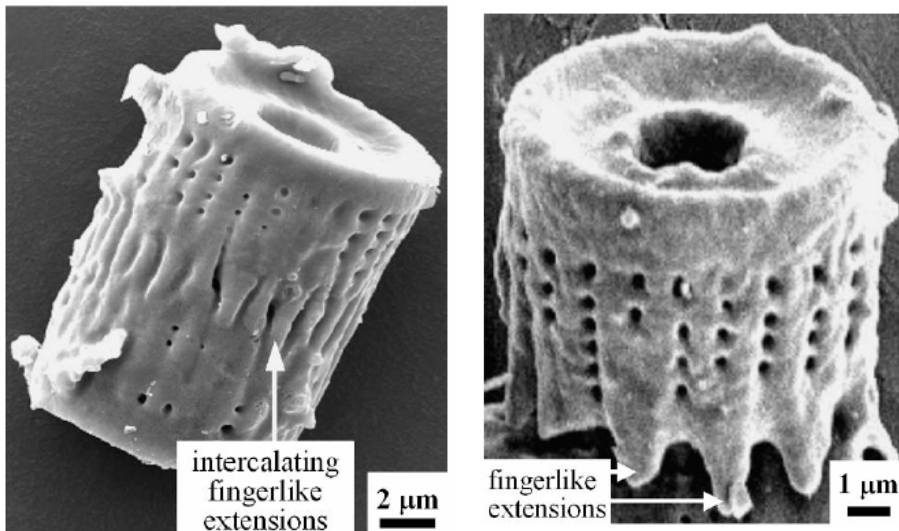
Electrochemical Deposition



Profiting from Biominerals Chemical Conversion of Diatoms

Shape-preserving conversion of SiO_2 -based diatom frustules into new structured materials

Diatoms \Rightarrow unique 3D morphologies, specific patterns of fine features
 \Rightarrow no synthetic analogues

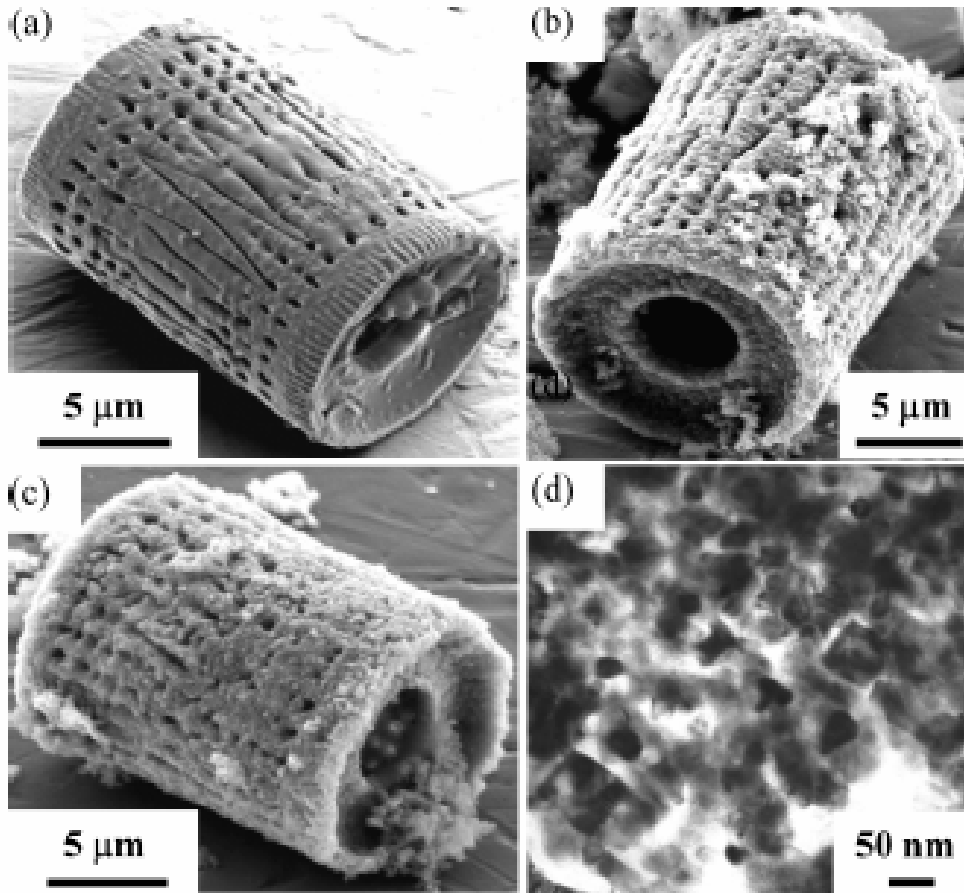


Used as precursors to a range of ceramics including:

TiO_2 , ZrO_2 , BaTiO_3

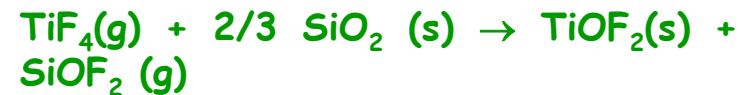
Silica-based *Aulacoseira* diatom

3-D Nanoparticle Structures from Anatase

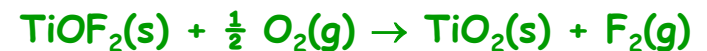


(a) Untreated diatom

(b) Exposure to TiF₄(g) 2h, 350°C

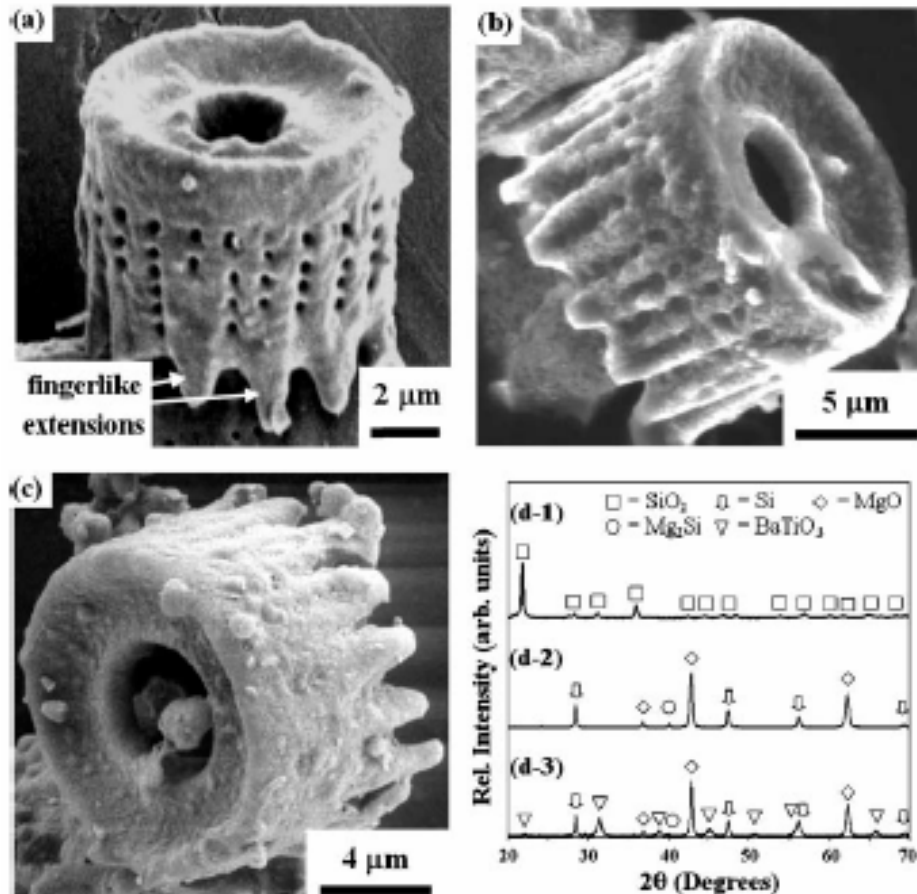


(c) Exposure to TiF₄(g) 2h at 350°C then pure O₂ for 2h at 350 °C.



(d) TEM image of cross-section of frustule after exposure to TiF₄(g) for 2 h, 350 °C and then to O₂ for 2h at 350°C.

Replication of Diatom Structure in BaTiO₃



(a) Diatom frustule

(b) After reaction with Mg(g) for 1.5 h at 900 °C



(c) A MgO-bearing frustule coated with a BaTiO₃ sol-gel precursor and fired at 700 °C for 1.5 h.

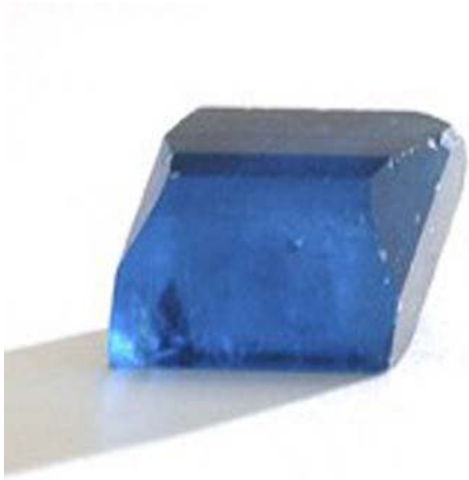
Layer of tetragonal BaTiO₃ formed on underlying scaffold containing MgO, Si, Mg₂Si

(d) XRD analyses of (a) (b) and (c)

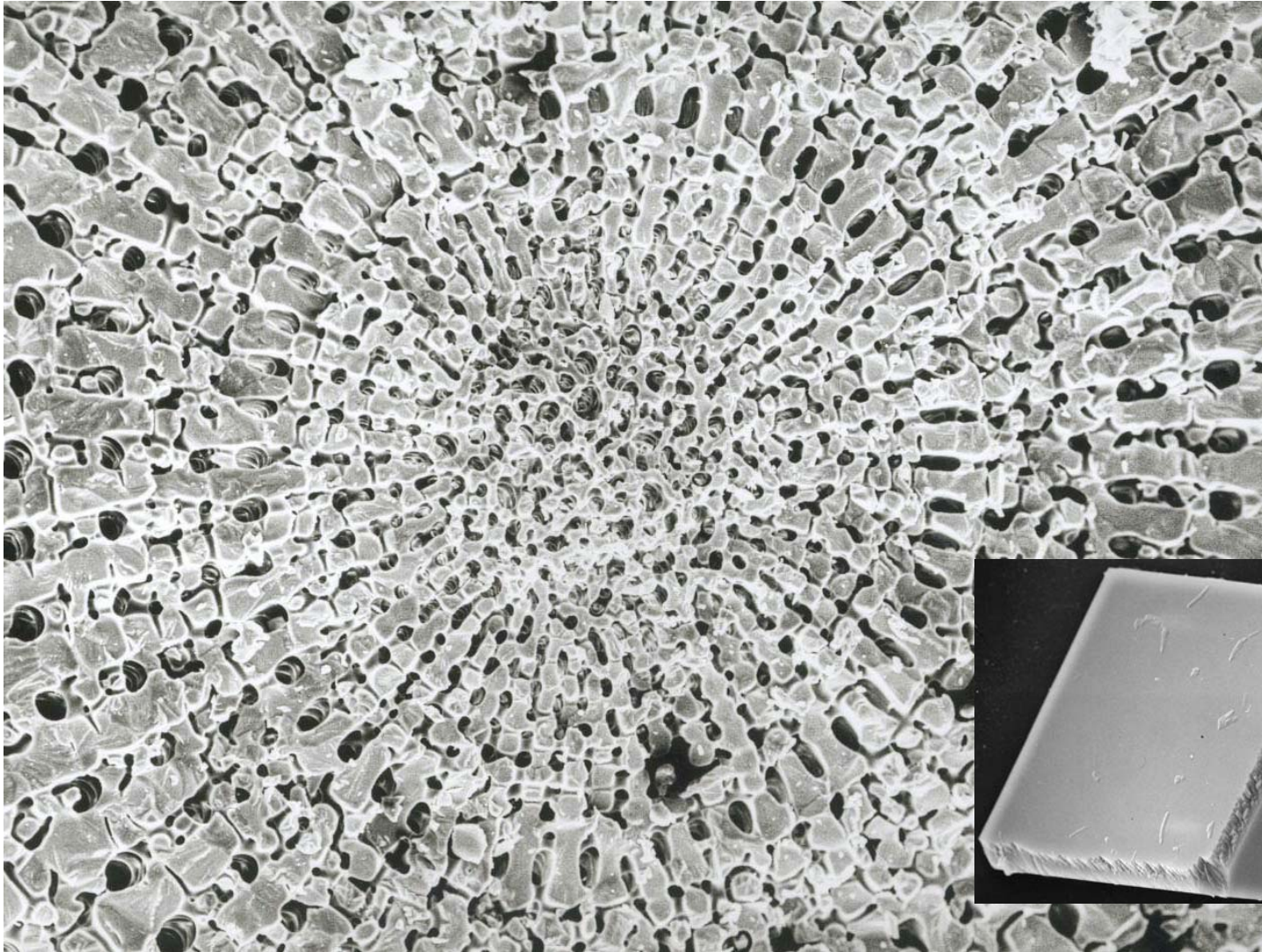
Templating Routes to Single Crystals with Complex Morphologies

- Nature shows it is possible to produce **calcite single crystals** with complex morphologies (eg. sea urchin plates)
- Clearly cannot use simple additives to produce such morphologies
- ⇒ biology forms such complex forms **within structured environments**
- Is it possible to produce **remarkable morphologies** in the absence of complex biological mechanisms by **shape constraint only** ?

Consider a "Single Crystal"....

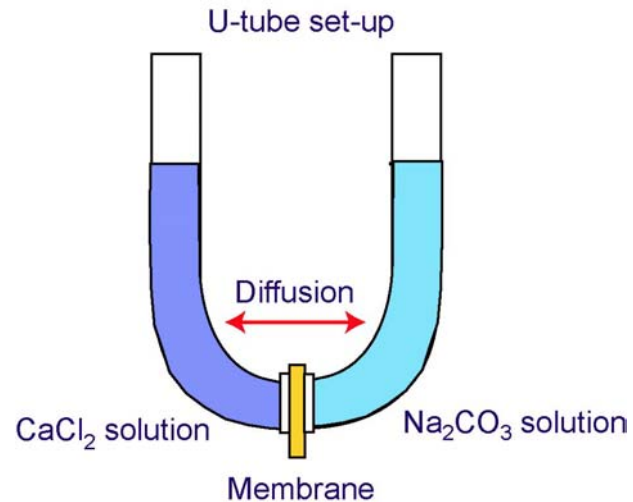
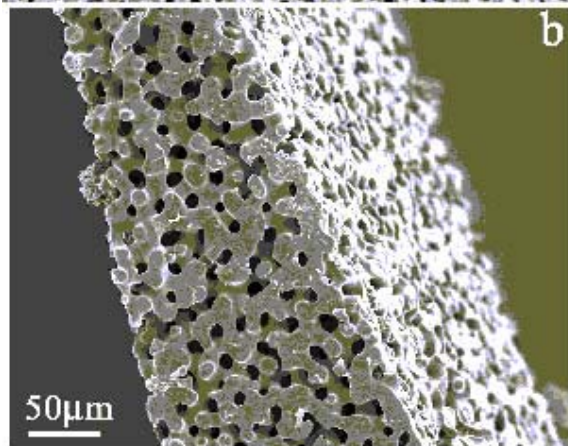
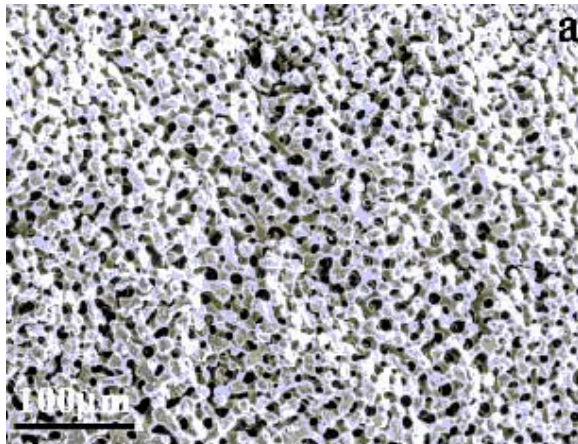


Now look at Biology...



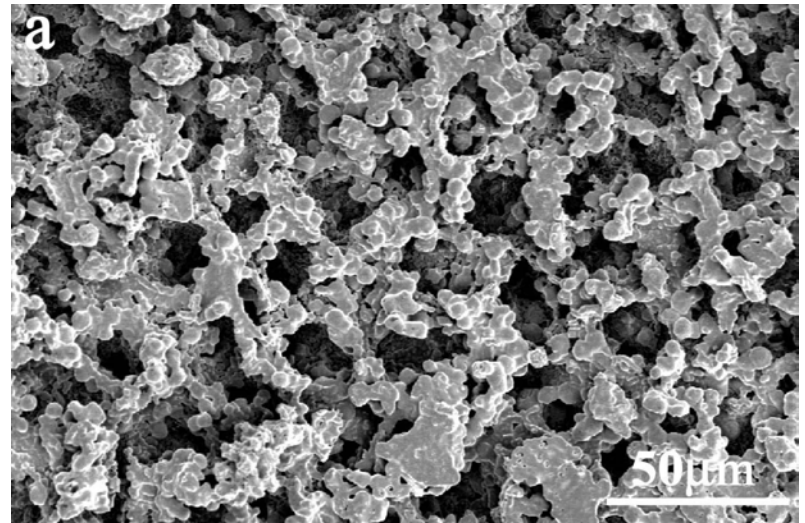
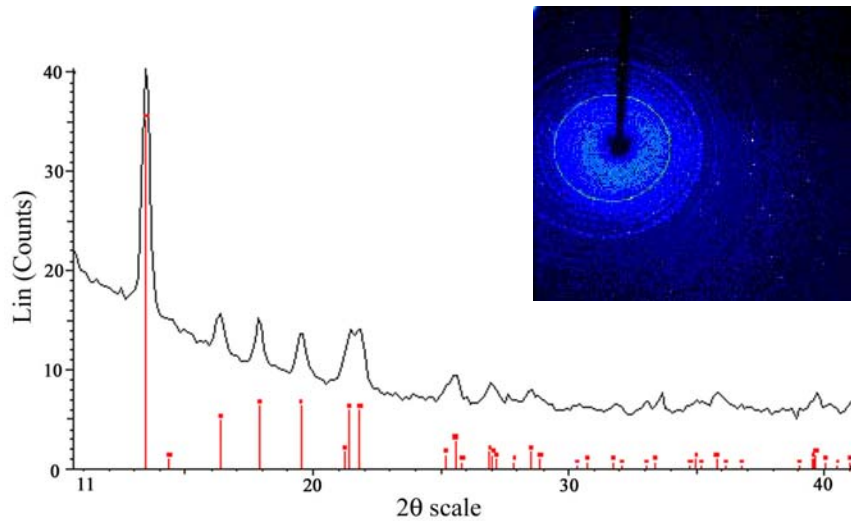
Calcium Carbonate Precipitation in Sponge-Like Polymer Membrane

CaCO_3 precipitation in sponge-like “sea urchin” membranes



- **Double-diffusion method**
- Mixing of Ca^{2+} and CO_3^{2-} in membrane results in precipitation of CaCO_3
- Product highly **concentration-dependent**

Polycrystalline Product

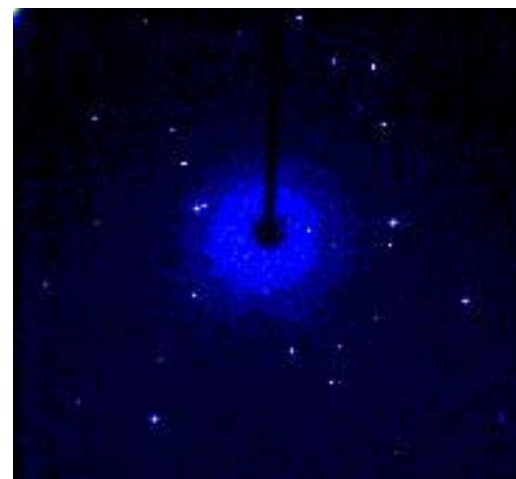
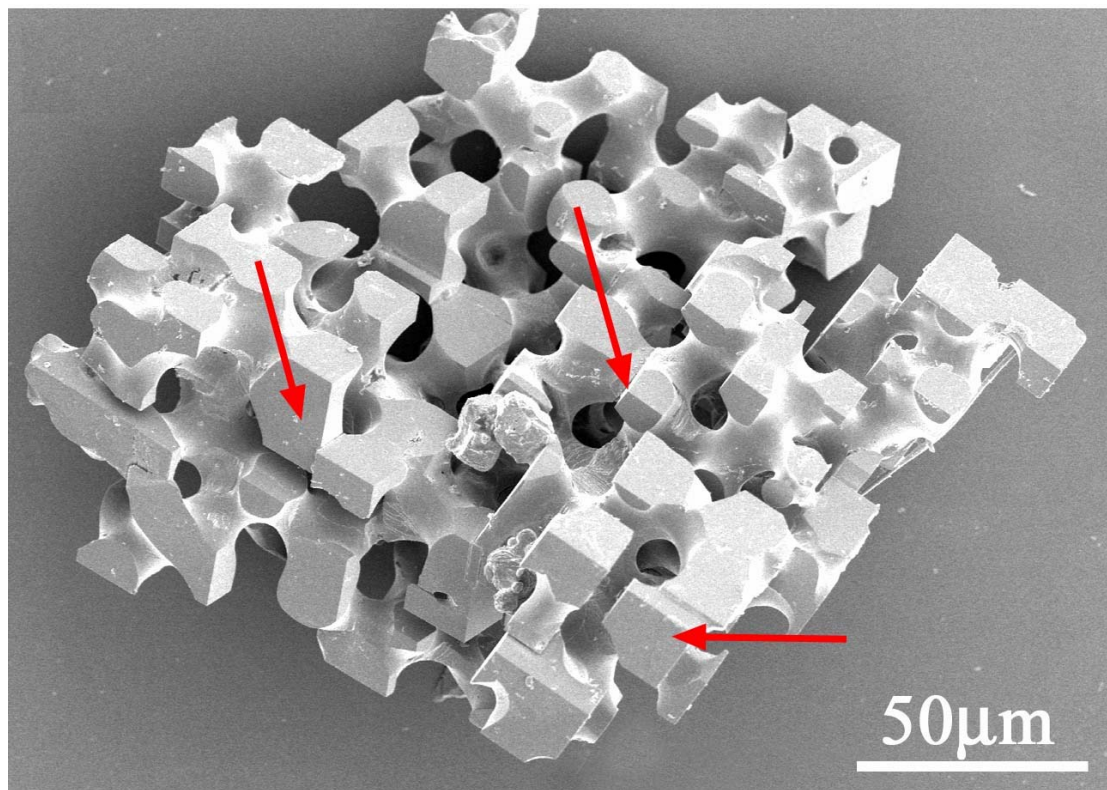


Reagents 0.1 M \Rightarrow evidence of templating
 \Rightarrow Product polycrystalline

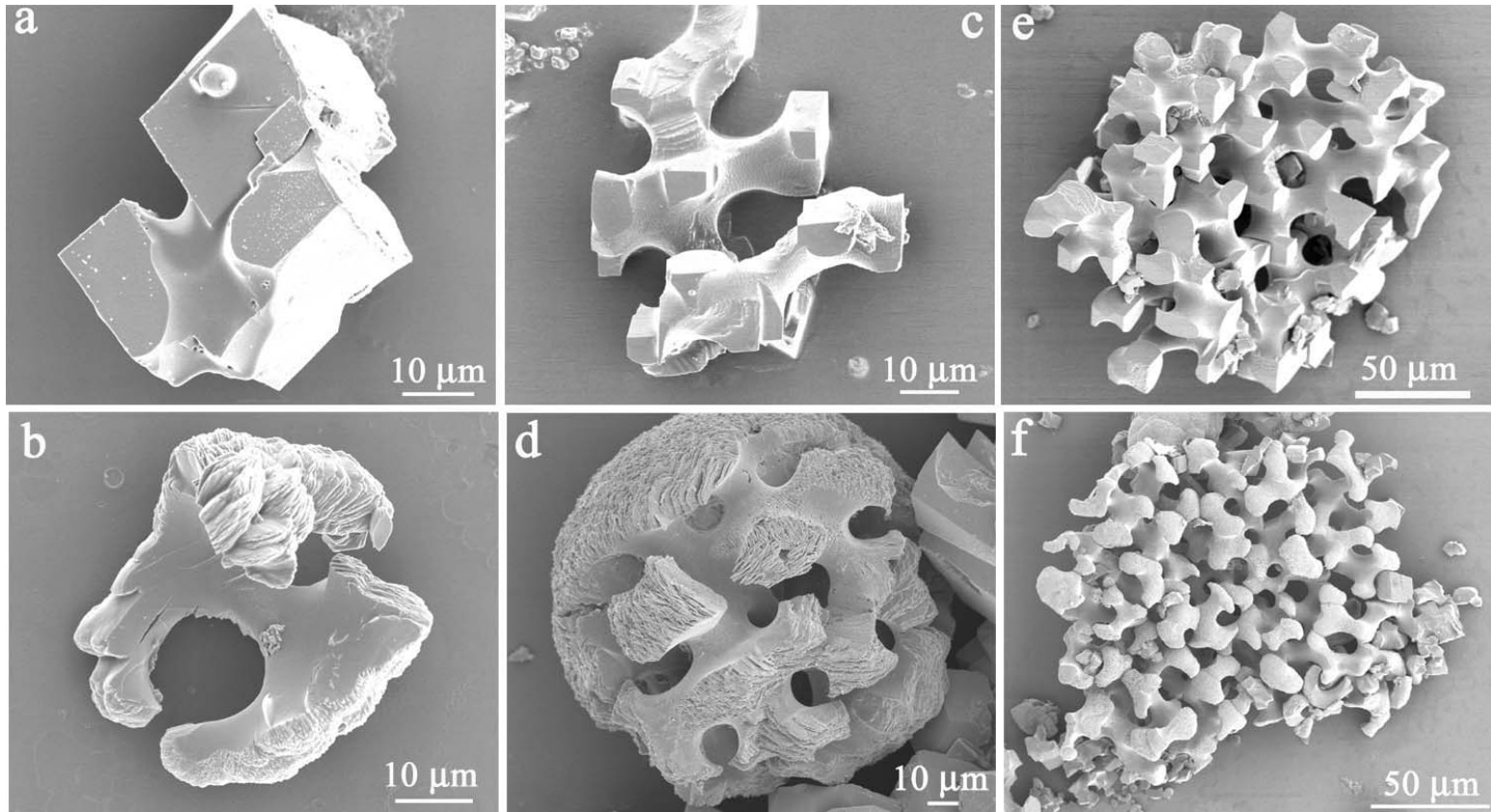
Single Crystal Product

Low concentration reagents (0.02 M)

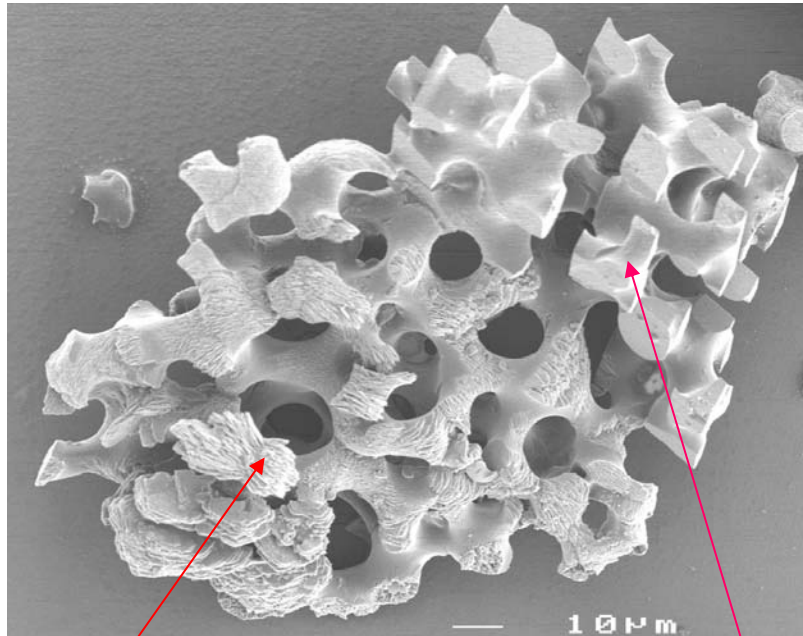
⇒ single crystals formed !!



Growth Mechanism



Calcite and vaterite particles precipitated initially in 1:1 ratio
24 hrs \Rightarrow 75% particles calcite



Vaterite

Calcite

Incubation Time	C : V Ratio	Particle Size μm
20 min	50%	20 - 30
1 hour	50%	60 - 80
2 hours	60%	90 - 110
1 day	75%	> 120
3 days	> 80%	> 120

- Proportion of calcite to vaterite **increases with time**
- **Dissolution** of vaterite \Rightarrow **reprecipitation** as calcite
- Larger particles \Rightarrow transformation of **vaterite to calcite**

Summary

- Experiments demonstrate it is possible to produce **calcite single crystals with complex morphologies** synthetically

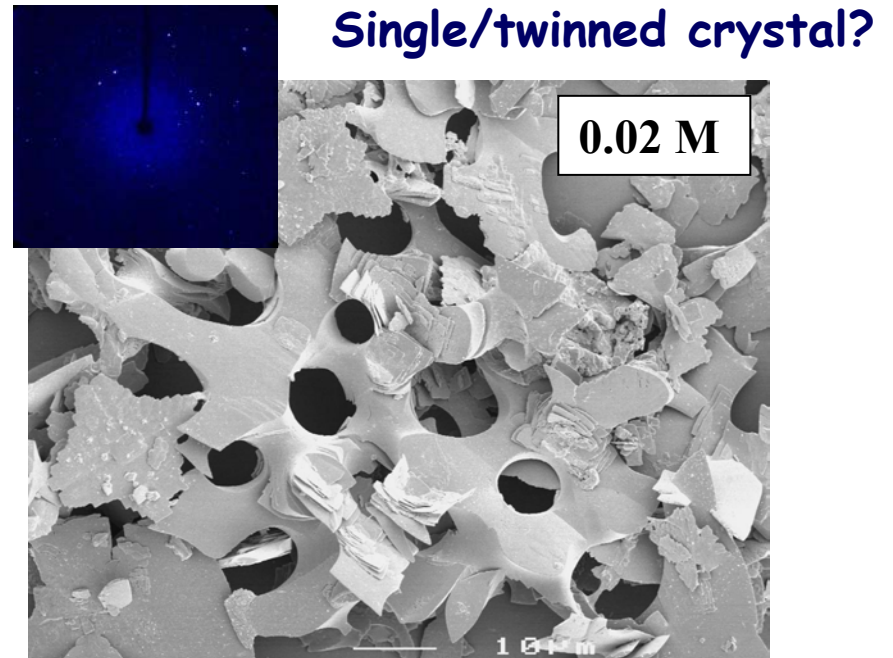
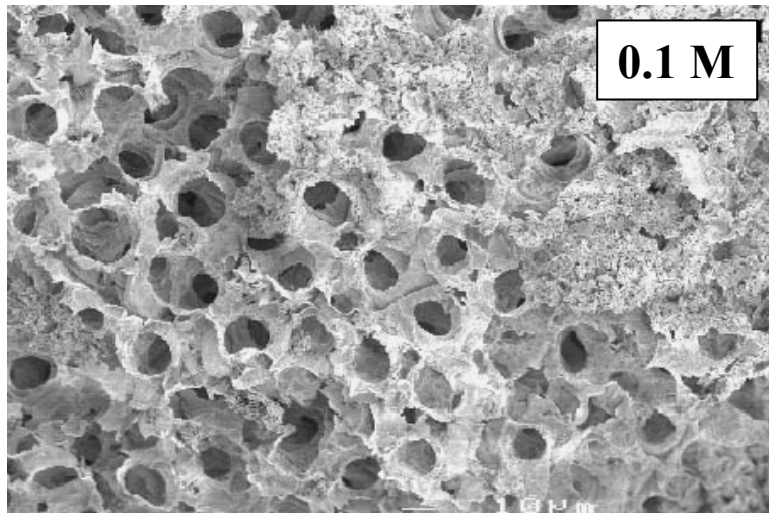
⇒ no elaborate control mechanisms are required

**CONSTRAINT OF MORPHOLOGY IS
SUFFICIENT**

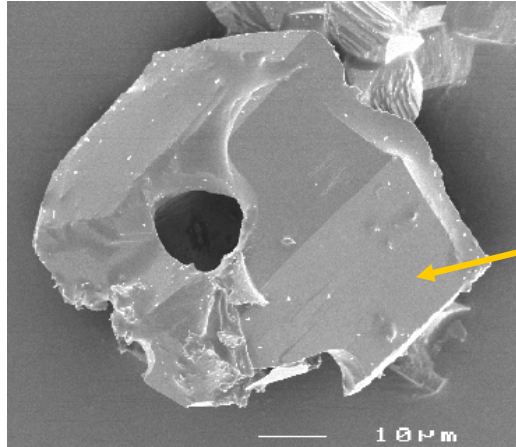
**Can A Similar Route Be Used To Template
Other Single Crystals ?**

Barium Sulphate

- Product **concentration dependent**
- High conc (0.1 M) clearly **polycrystalline**
- Low conc (0.02 M) tends to **templated single crystals**

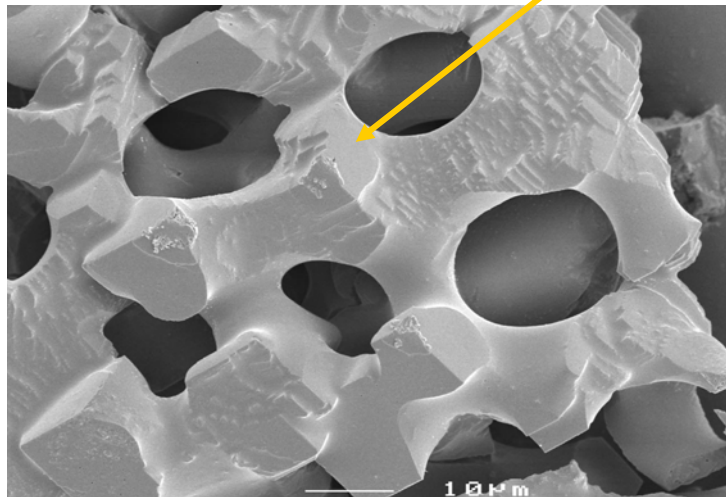


Strontium Sulphate

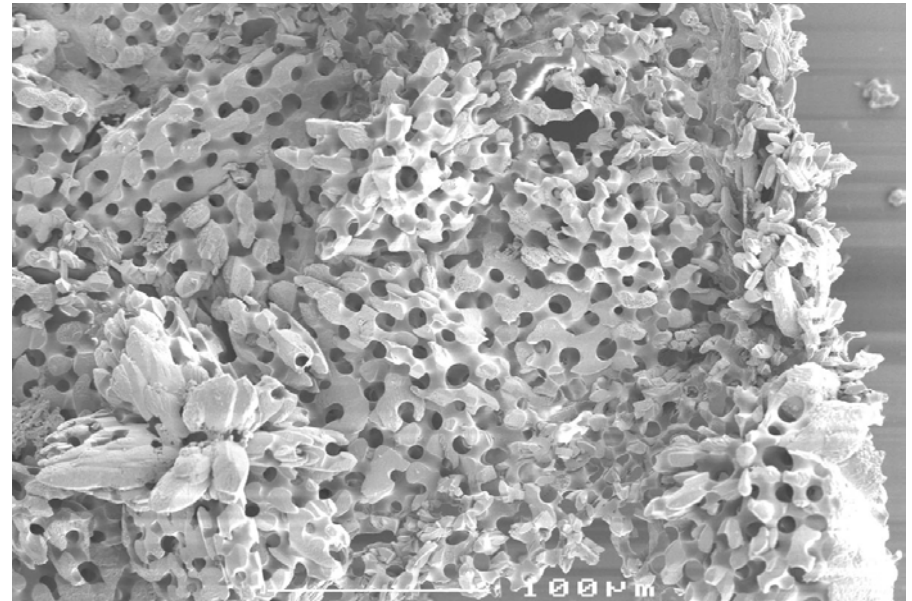


0.1M SrCl_2
for 4hr

Well-defined crystal faces
indicate **single crystal**
character

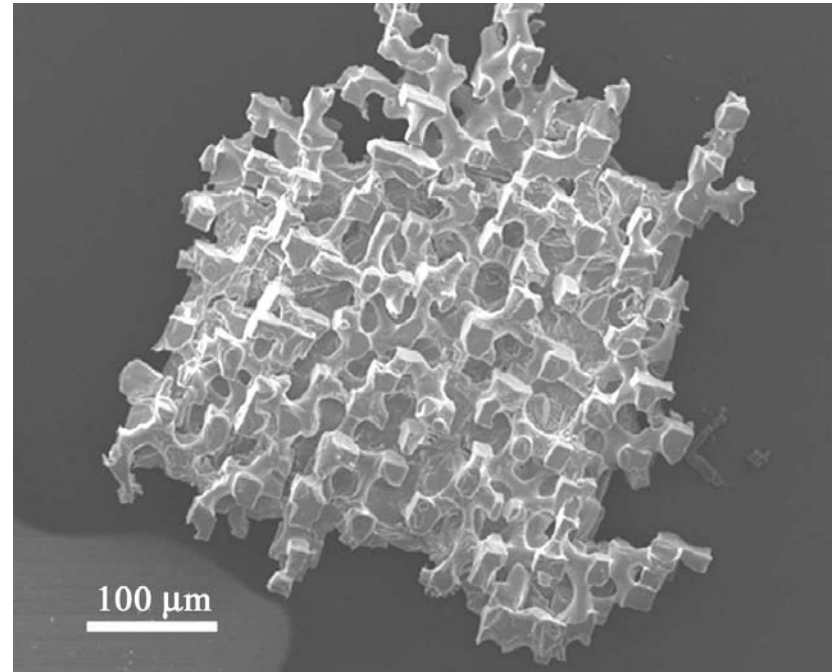
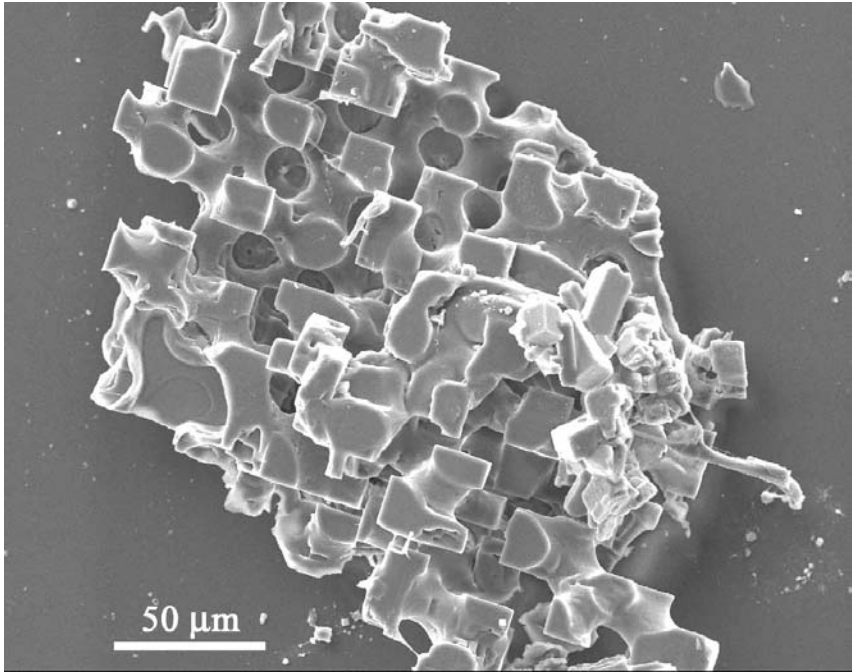


0.02 M SrCl_2 for 24 hr



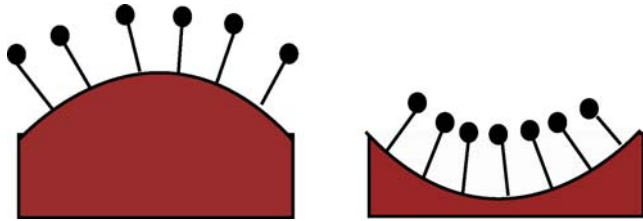
0.1M SrCl_2 for 24 hrs
MANY SINGLE CRYSTALS

Sodium Chloride

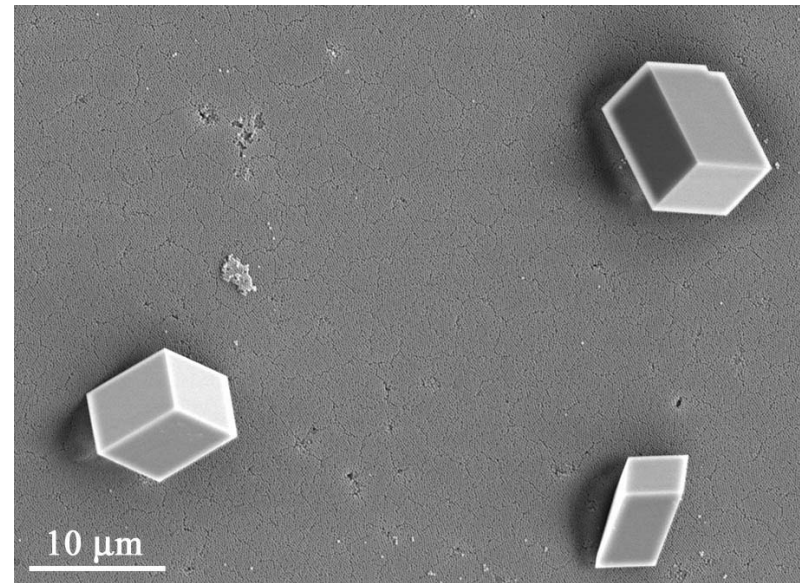
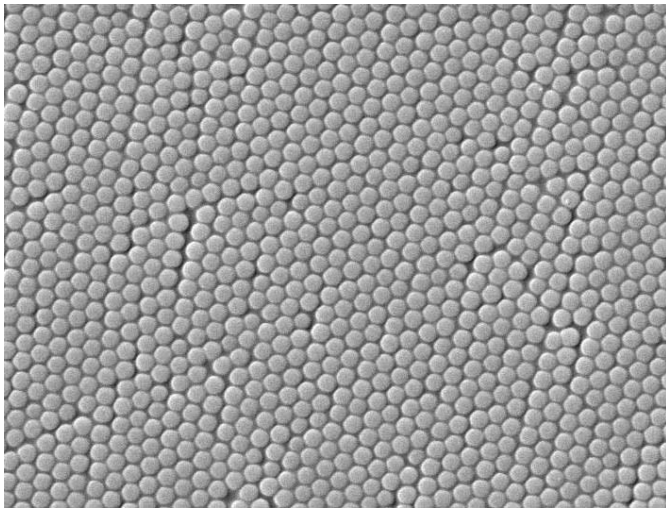


NaCl crystals formed by **evaporation of a saturated solution**

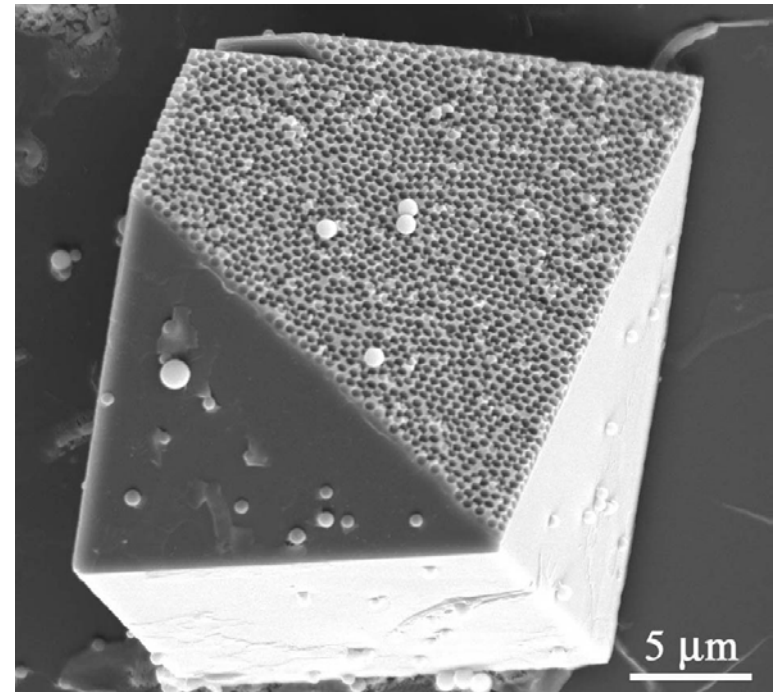
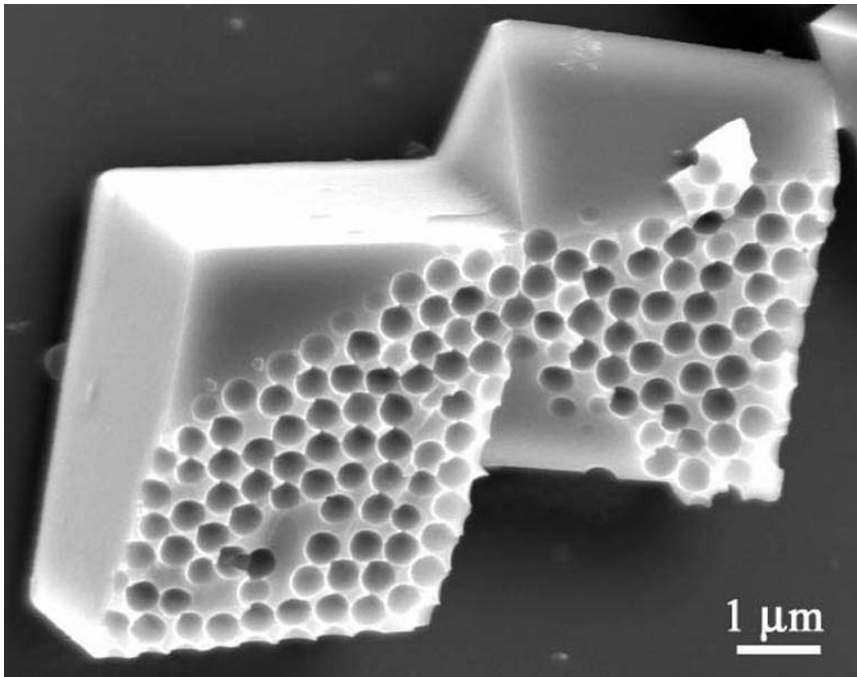
Surfaces with Well-Defined Topography



- Construct SiO_2 or polystyrene particle monolayers
- CaCO_3 grown on monolayers

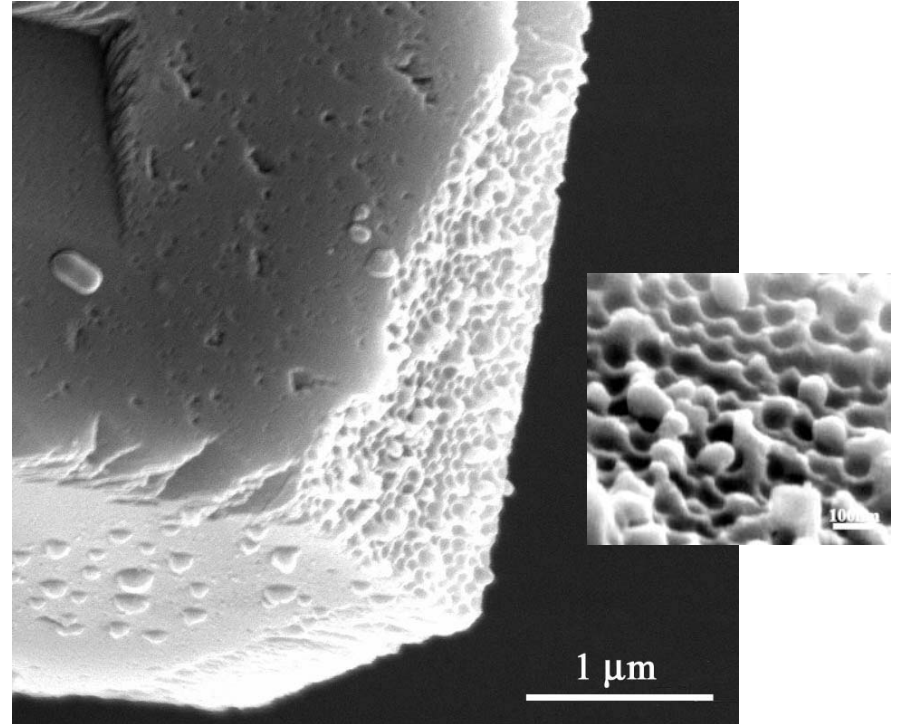
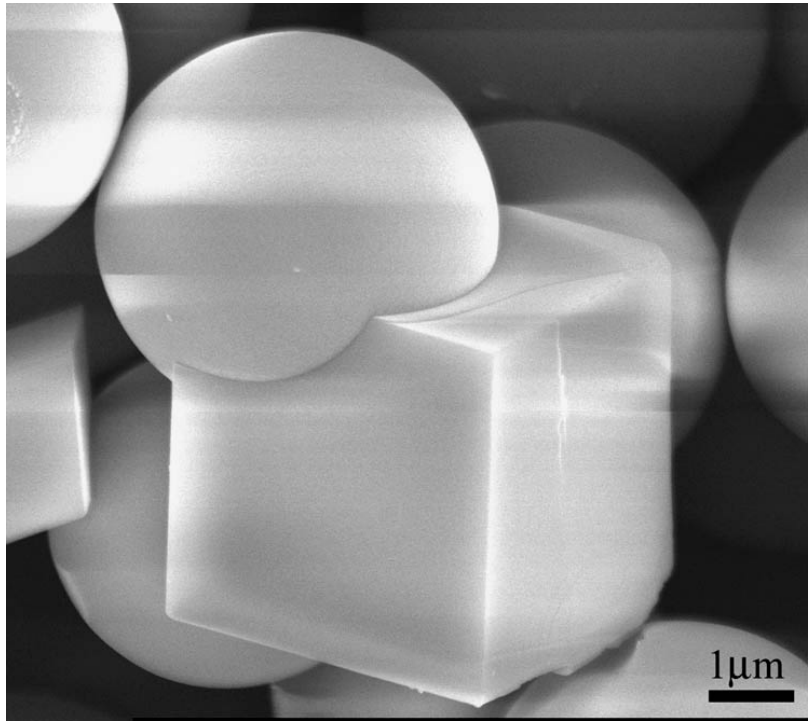


Nucleating Crystal Face Templated by Monolayer



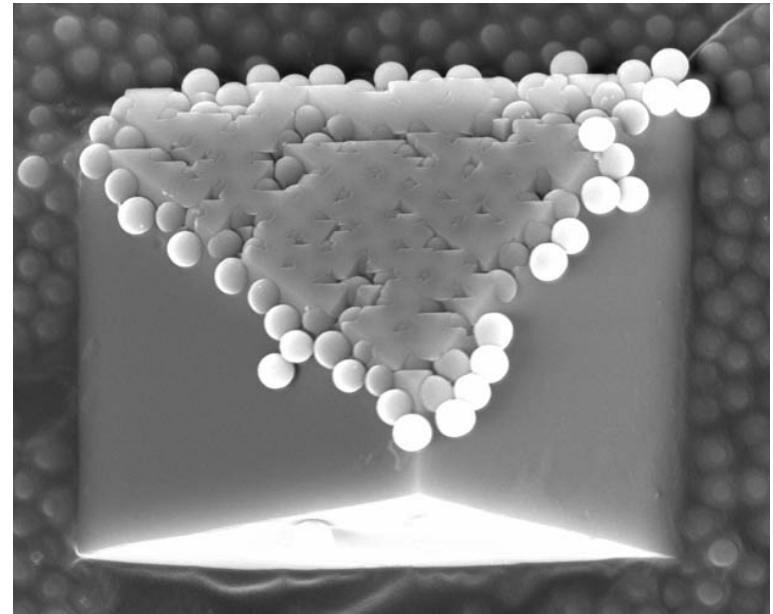
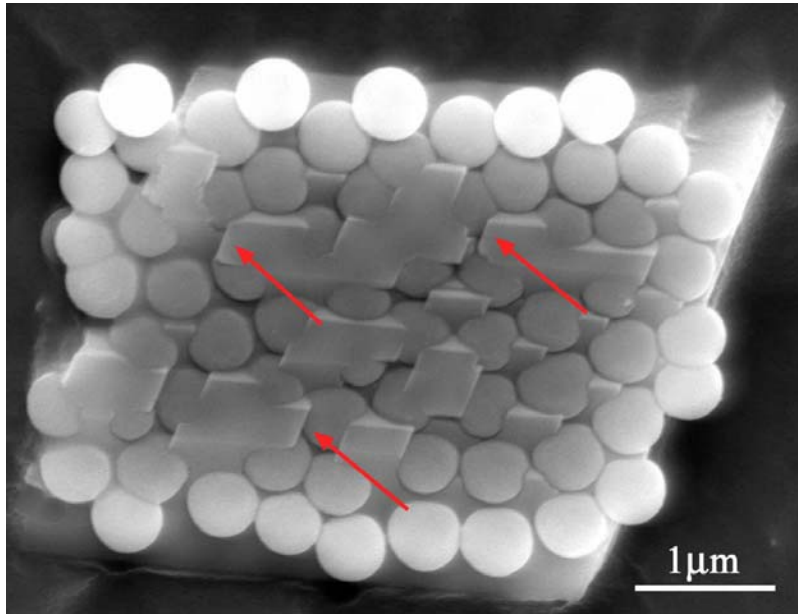
Calcite crystals grow around particles → shape of particles perfectly reproduced in single crystal

Influence of Particle Size ...



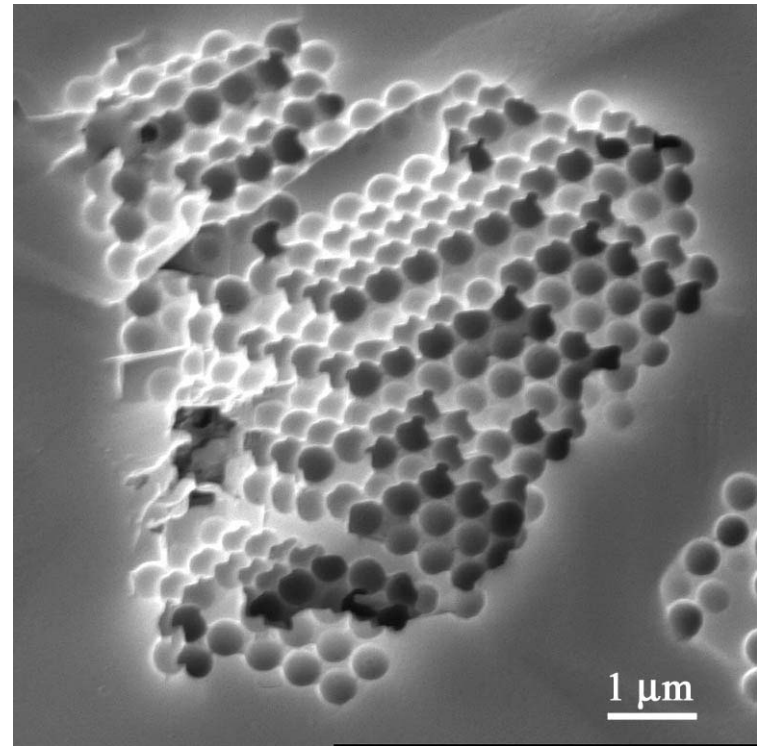
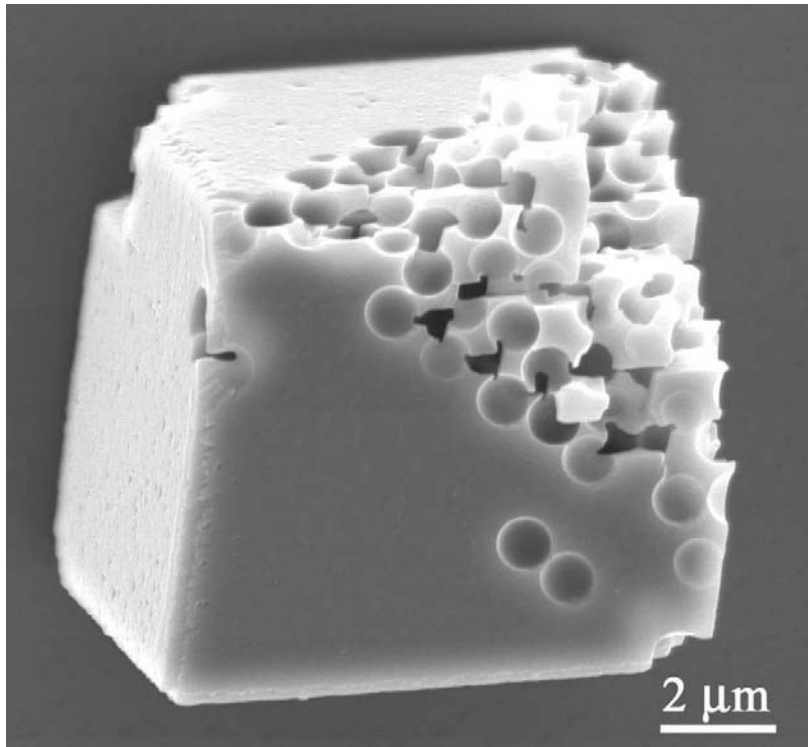
Templating successful in particle size range **5 μm to 50 nm**

Continued Growth..



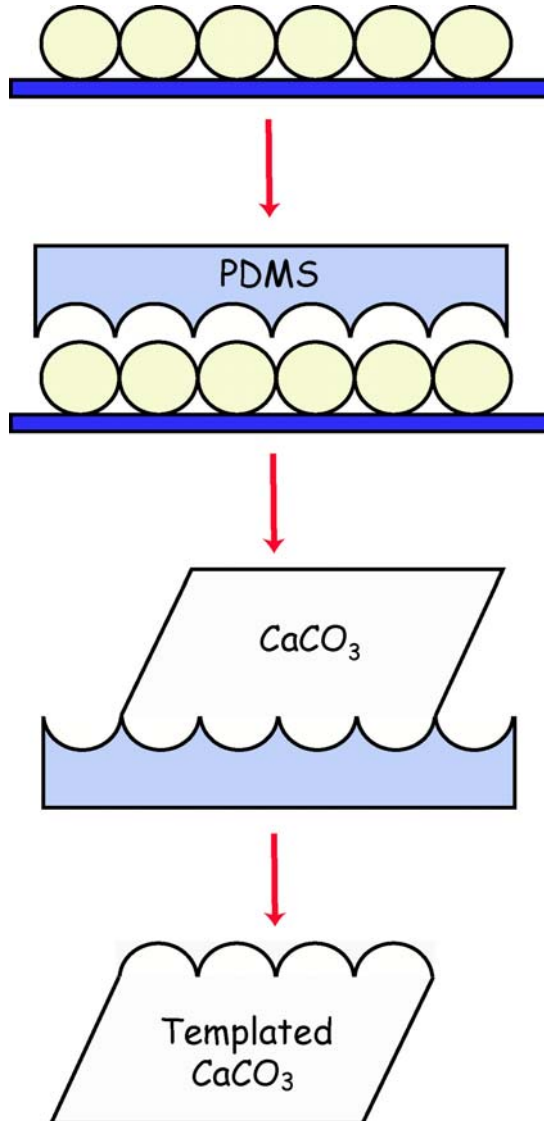
- Allow crystal growth to continue - see growth *through* the colloidal monolayer
- Particles become **encapsulated within single crystals**

Crystal Growth on Colloidal Multilayers



Can extend methodology to use **colloidal multilayers** and form crystals **templated in 3D**

Surfaces with Positive Curvature

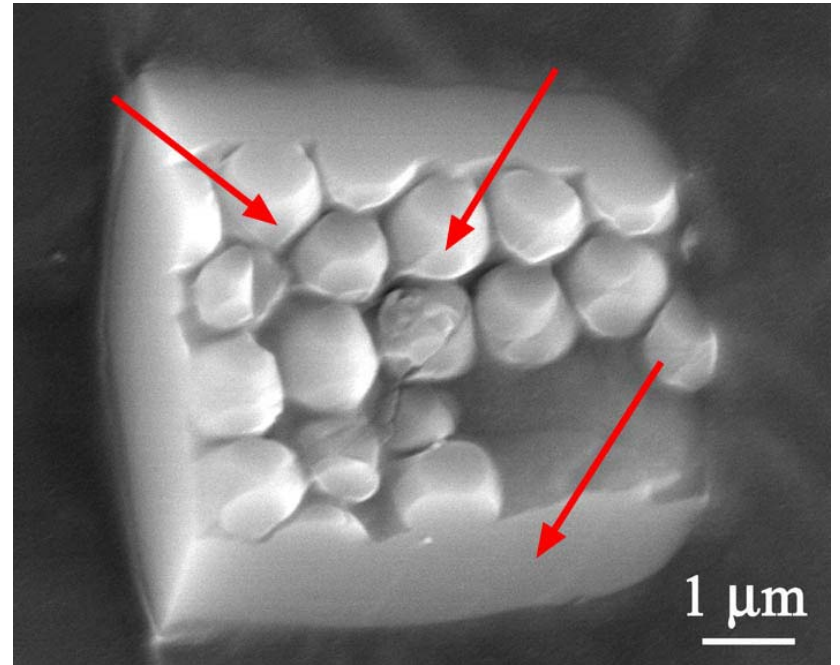
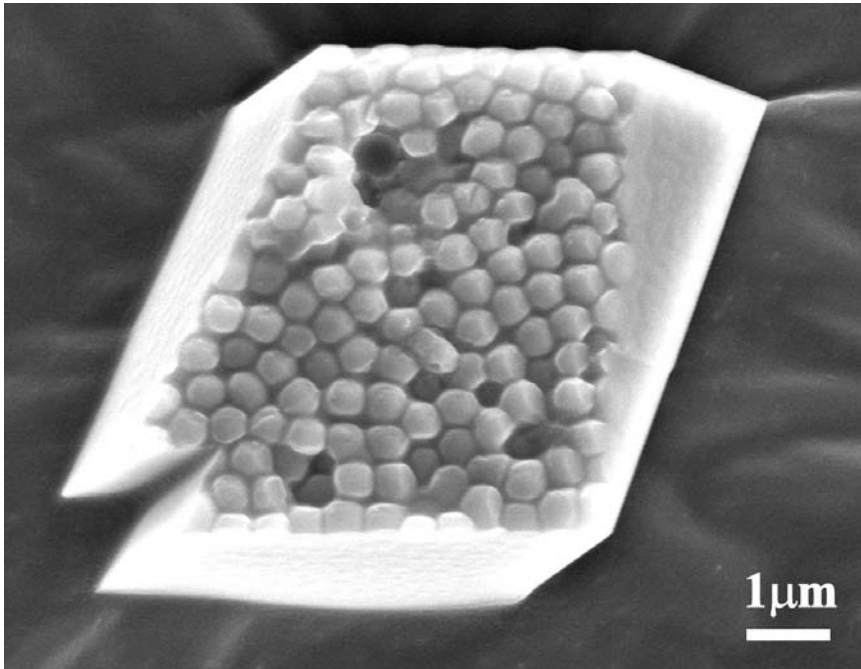


- Surfaces of opposite curvature created by generating PDMS replica of particle monolayer

- CaCO_3 precipitated on PDMS replica

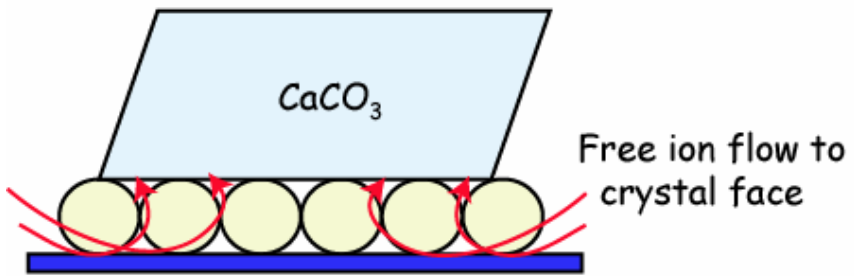
... Templated Crystals Produced

- Again see replication of template pattern in crystal face

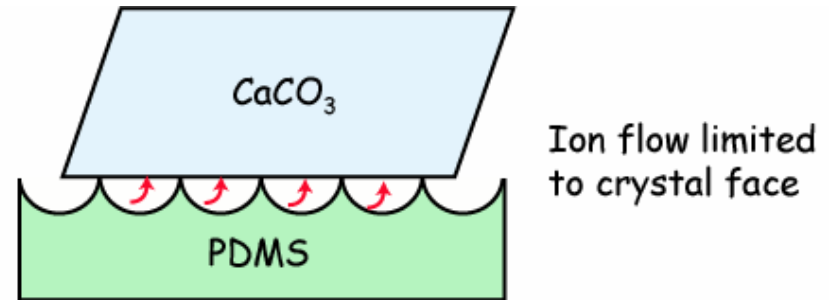
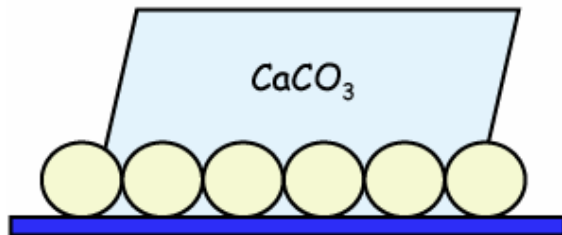


- As opposed to perfectly smooth surfaces, see evidence of defined crystal faces

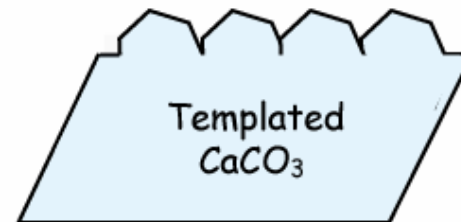
... Mechanism



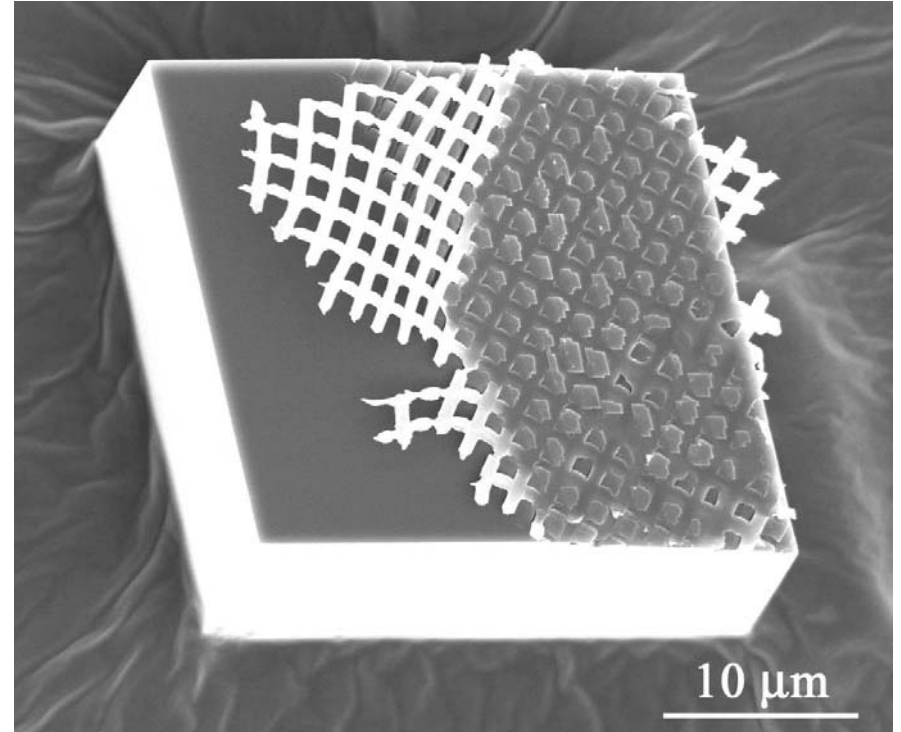
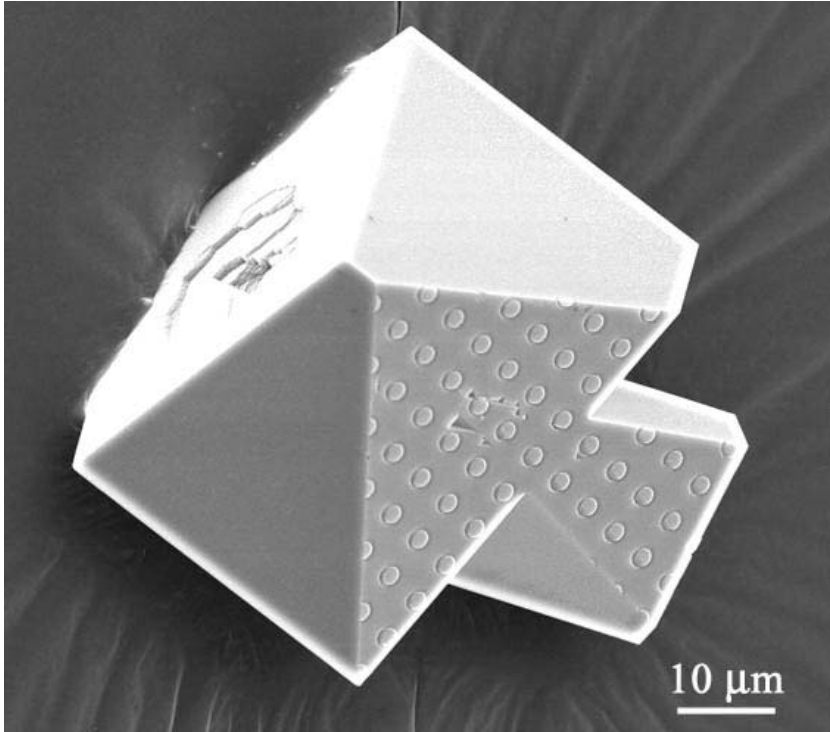
Growth through monolayer



Growth not limited by template



Polymer Film Templates

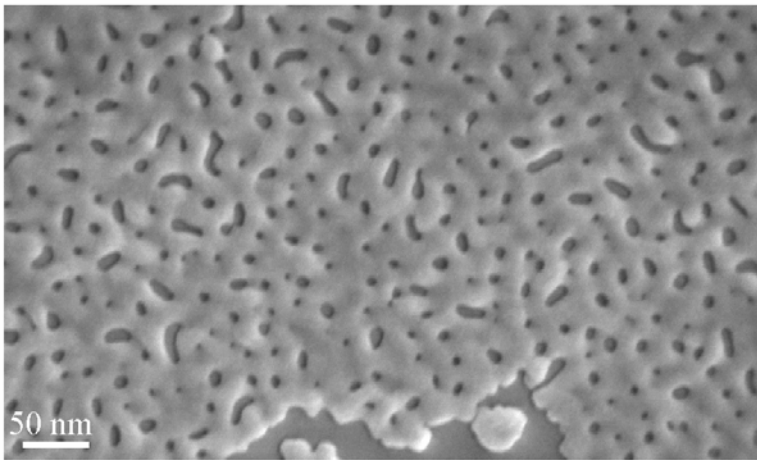


Using **patterned polymer films** to template crystal surfaces
⇒ Potential for structuring surfaces at **small length scales**

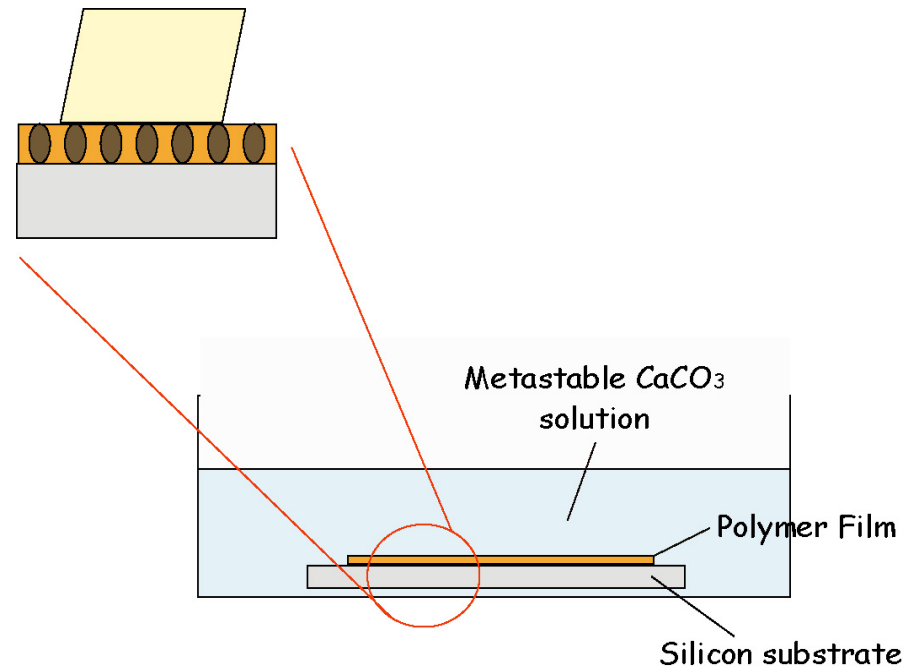
Sabine Ludwigs, Ulli Steiner, University of Cambridge

Patterning at Small Length Scales

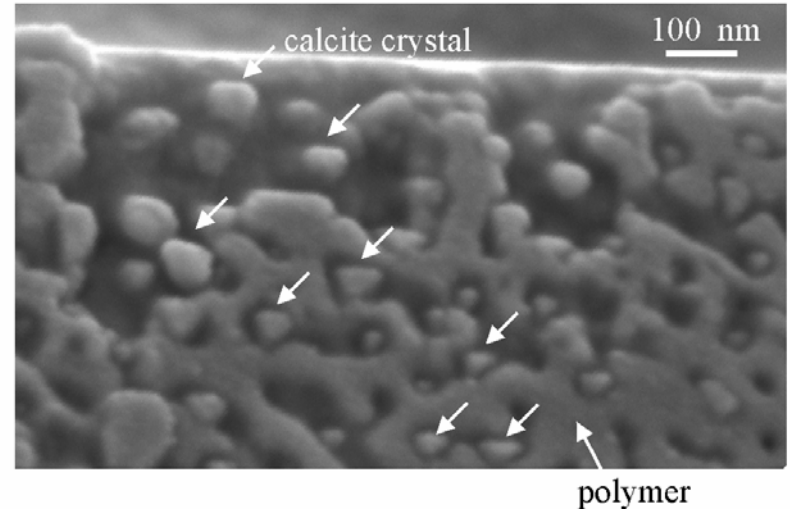
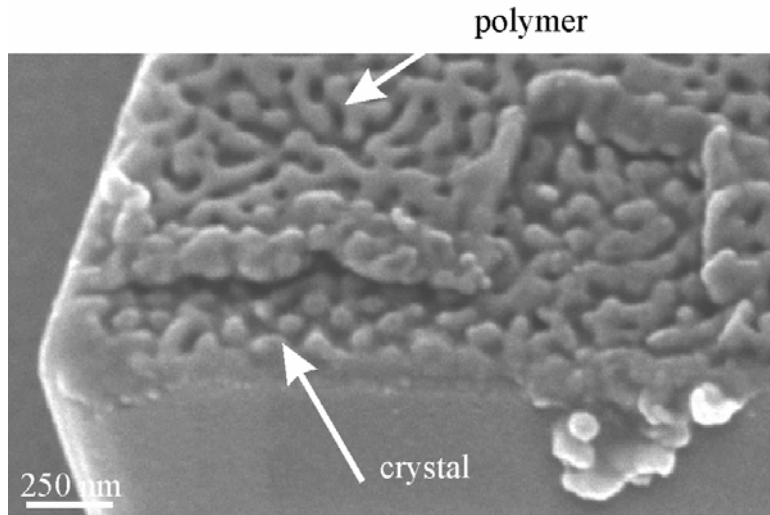
Demixing of polymer blends and subsequent removal of one component polymer templates yields patterned films with structure sizes from 100 nm - 10 nm prepared.



porous polystyrene film prepared via spontaneous phase separation of a polystyrene / polymethylmethacrylate blend and selective removal of PMMA



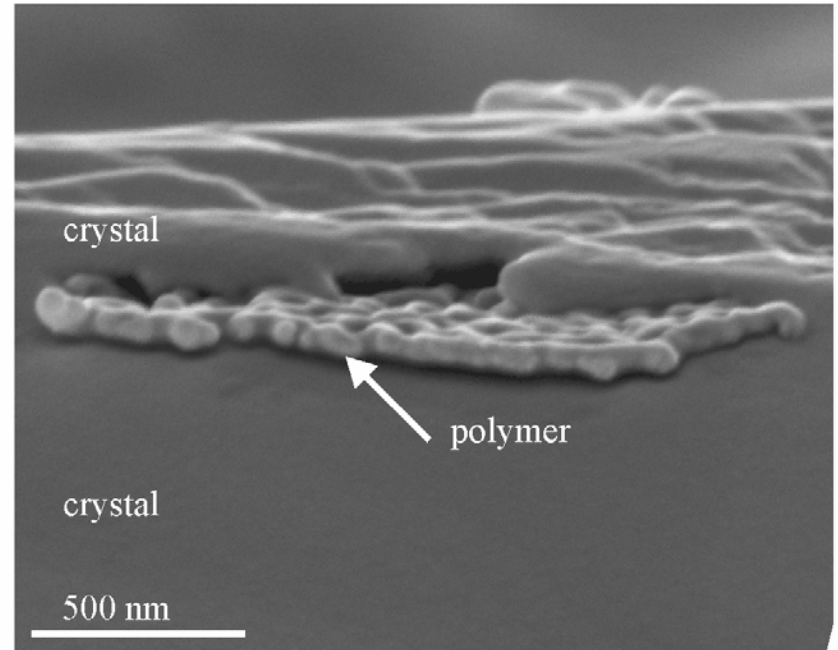
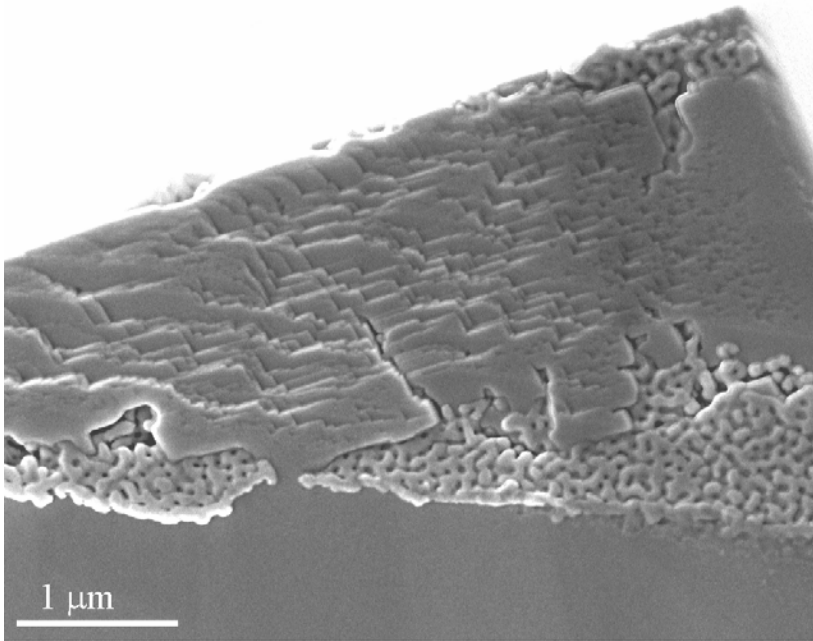
Crystal Growth on Polymer Film



- Crystals nucleate on the surface of the polymer film
- Removal of the crystals from the substrate reveals the crystal face which nucleated on the polymer film
- Separation of the polymer shows the crystal morphology to be templated by the polymer film

Continued Growth ...

Through Pores in Polymer Film

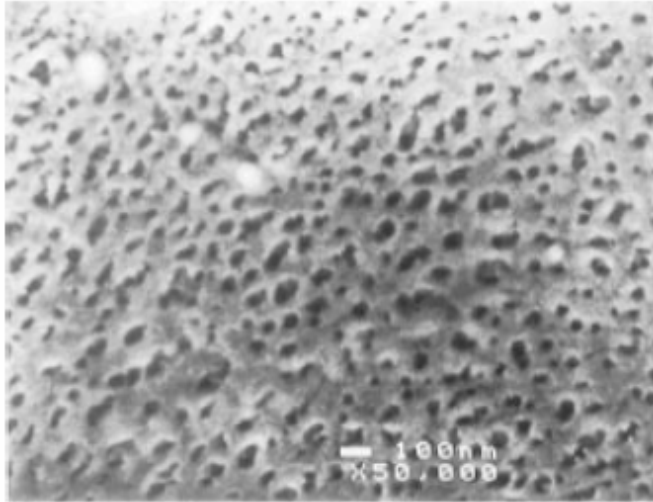


Further crystal growth results in **growth through the pores**

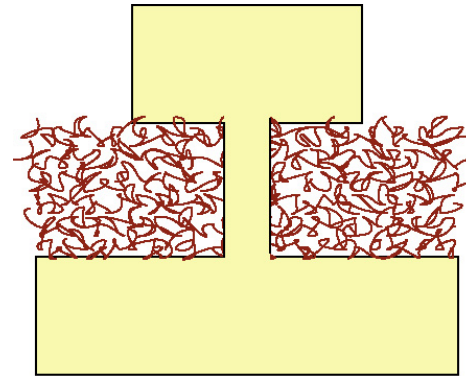
⇒ Continued on other side of polymer film

⇒ Polymer film becomes incorporated in the crystal

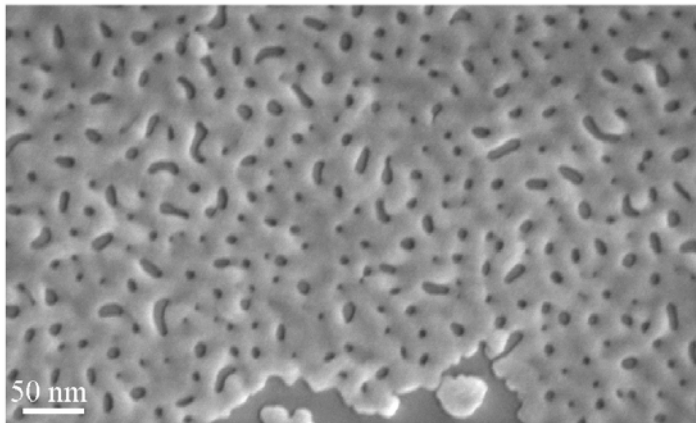
Reminiscent of Abalone Nacre ?



Abalone polymer film



MINERAL BRIDGES

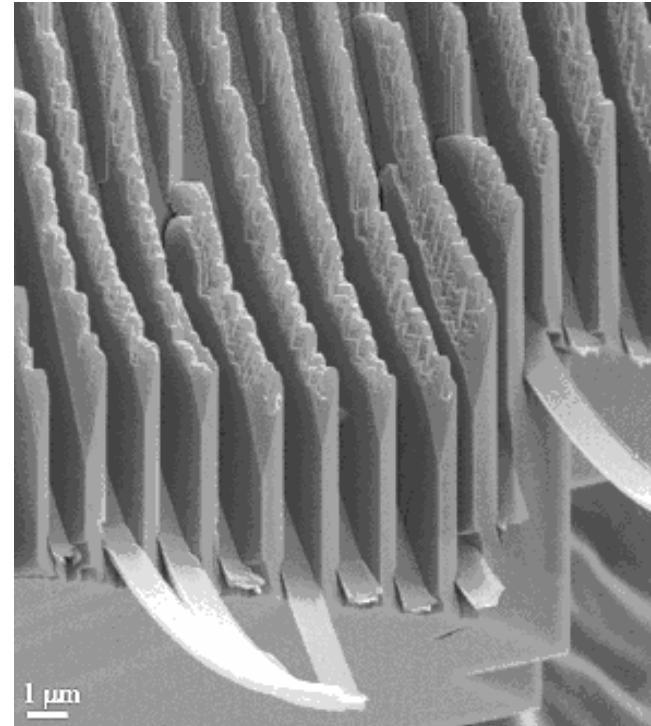
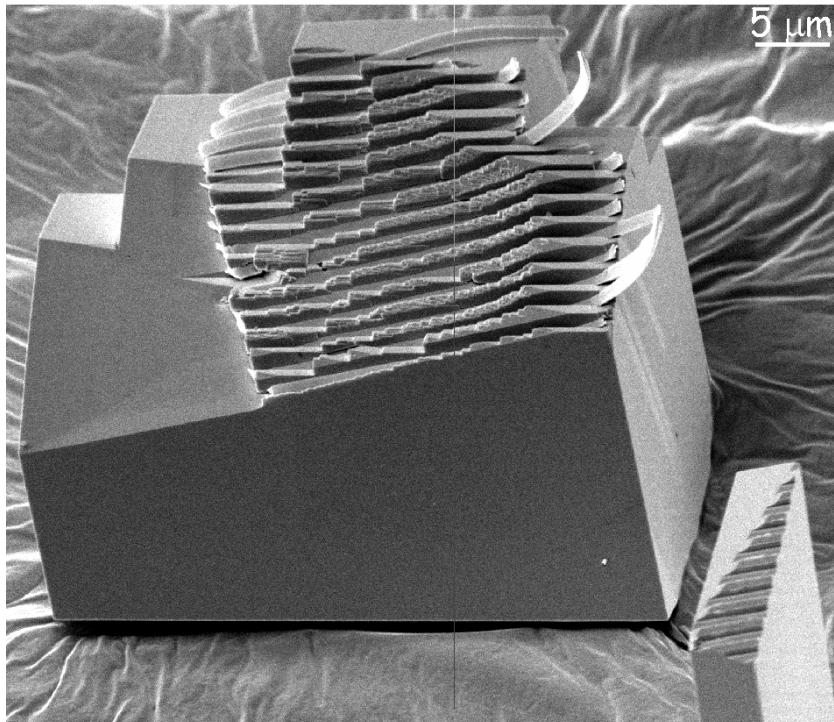


Synthetic polymer film

Structure of nanoporous polymer thin film and crystal growth through strongly resemble abalone nacre

⇒ Further vindication for this model?

High Aspect Ratio Crystal via Patterning with Polymer Thin Film



Control of crystal growth using a polymer mask. Directional growth in the area not covered by the polymer (thin stripes), giving rise to a **high aspect ratio morphology of the crystal.**

Summary

Controlling Crystal Morphologies:

- Additives to control single crystal morphologies
 - ⇒ Subtle changes in morphology/ mechanism controversial
- Additives to produce polycrystalline structures
 - ⇒ Oriented and non-oriented structures
 - ⇒ Block copolymers extremely versatile
- Templating to control production :
 - ⇒ Nanoparticles / ferritin and virus cages
 - ⇒ Polycrystalline structures with complex morphologies
 - ⇒ Single crystals with complex morphologies
 - / simple templating sufficient!